Government of Western Australia

Department of
Mines and Petroleum

REPORT
170

ASSESSMENT OF THERMAL MATURITY USING BITUMEN, GRAPTOLITE AND BIOCLAST REFLECTANCE: ORDOVICIAN NAMBEET FORMATION, OLYMPIC 1, CANNING BASIN

by LM Dent and LS Normore

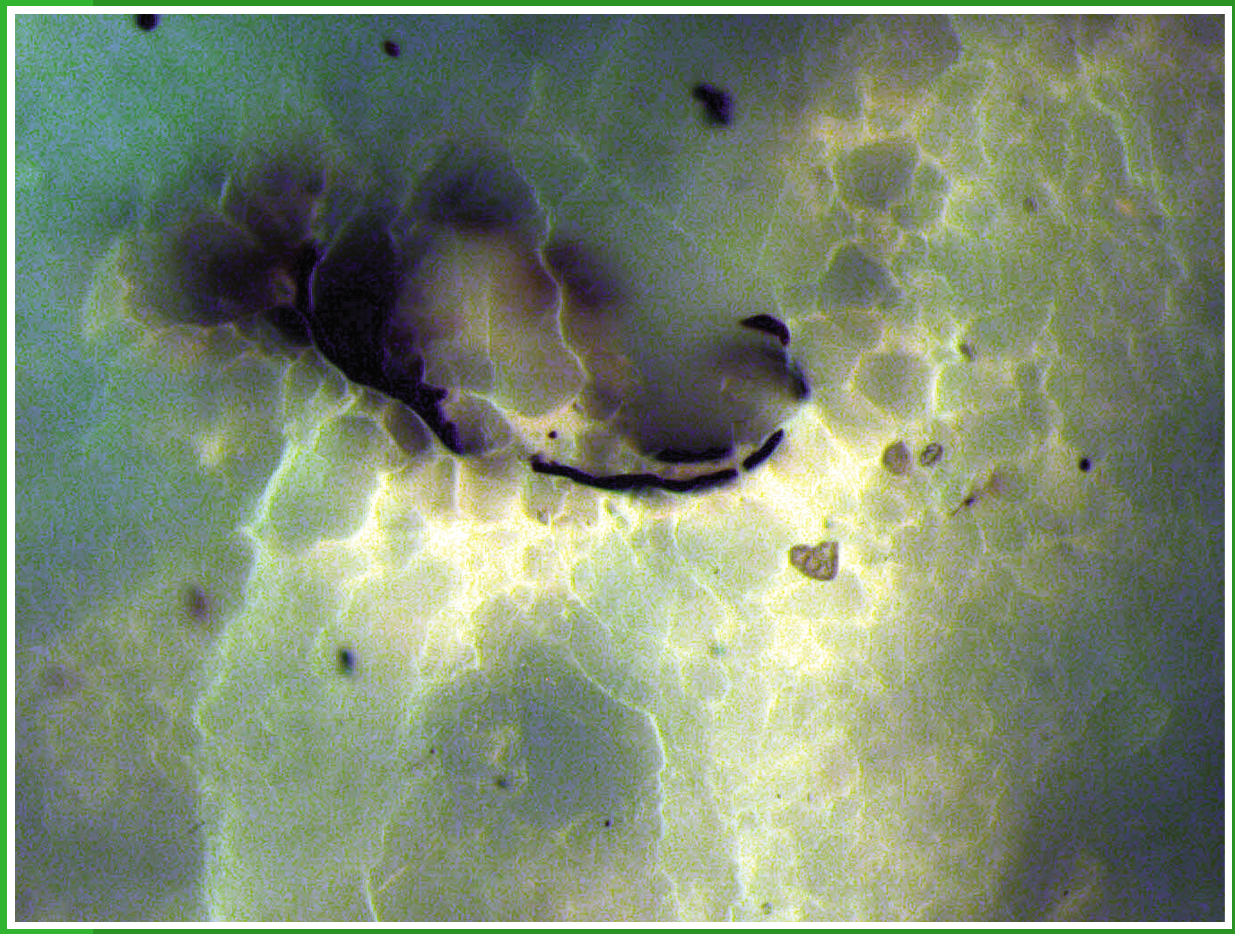

EXPLORATION INCENTIVE SCHEME

Geological Survey of Western Australia

Government of Western Australia
Department of Mines and Petroleum

REPORT 170

ASSESSMENT OF THERMAL MATURITY USING BITUMEN, GRAPTOLITE AND BIOCLAST REFLECTANCE: ORDOVICIAN NAMBEET FORMATION, OLYMPIC 1, CANNING BASIN

by
LM Dent and LS Normore

Perth 2017

Geological Survey of
Western Australia

MINISTER FOR MINES AND PETROLEUM
Hon Bill Johnston MLA

ACTING DIRECTOR GENERAL, DEPARTMENT OF MINES AND PETROLEUM
David Smith

EXECUTIVE DIRECTOR, GEOLOGICAL SURVEY OF WESTERN AUSTRALIA
Rick Rogerson

REFERENCE
The recommended reference for this publication is:
Dent, LM and Normore, LS 2017, Assessment of thermal maturity using bitumen, graptolite and bioclast reflectance: Ordovician Nambeet Formation, Olympic 1, Canning Basin: Geological Survey of Western Australia, Report 170, 21p.

National Library of Australia Cataloguing-in-Publication entry:

Creator:	Dent, L.M., author.
Title:	Assessment of thermal maturity using bitumen, graptolite and bioclast reflectance: Ordovician Nambeet Formation from Olympic 1, Canning Basin / LM Dent and LS Normore.
ISBN:	9781741687460 (ebook)
Subjects:	Petroleum--Prospecting--Western Australia--Canning Basin. Petroleum--Geology--Western Australia--Canning Basin. Sedimentation and deposition--Western Australia--Canning Basin.
Other Creators/Contributors:	Normore, L., author. Geological Survey of Western Australia, issuing body.

ISSN 0508–4741

Grid references in this publication refer to the Geocentric Datum of Australia 1994 (GDA94). Locations mentioned in the text are referenced using Map Grid Australia (MGA) coordinates, Zones 51 and 52. All locations are quoted to at least the nearest 100 m.

Copy editor: SR White
Cartography: AK Symonds
Desktop publishing: RL Hitchings

Published 2017 by Geological Survey of Western Australia
This Report is published in digital format (PDF) and is available online at <www.dmp.wa.gov.au/GSWApublications>.

Further details of geological publications and maps produced by the Geological Survey of Western Australia are available from:
Information Centre
Department of Mines and Petroleum
100 Plain Street
EAST PERTH WESTERN AUSTRALIA 6004
Telephone: +61 8 9222 3459 Facsimile: +61 8 9222 3444
www.dmp.wa.gov.au/GSWApublications

EXPLORATION INCENTIVE SCHEME

Cover photograph: Bioclast viewed at 50x magnification in fluorescent mode

Contents

Appendix

Figures

Tables

Assessment of thermal maturity using bitumen, graptolite and bioclast reflectance: Ordovician Nambeet Formation, Olympic 1, Canning Basin

by

LM Dent and LS Normore

Abstract

In the absence of vitrinite, bitumen and zooclasts are used to derive vitrinite-equivalent reflectance values for the Ordovician Willara and Nambeet Formations in the Olympic 1 well, Canning Basin. These values are compared to vitrinite-equivalent reflectance values derived from T_{max} values recorded in the same well to assess thermal maturity.

For each particle type, bitumen or zooclast, raw reflectance values were transformed to a vitrinite-equivalent reflectance using multiple equations to cross-check the reliability of each equation and reduce the range of uncertainty of the thermal maturity results. The resulting vitrinite-equivalent reflectance ranges varied with particle type: bitumen BR_o = 0.9 – 1.2%, graptolite fragments GR_o = 1.4 – 1.7%, and bioclasts BCR_o = 1.0 – 1.5%. Bioclast and bitumen data showed good agreement in reflectivity values, and therefore thermal maturity, placing the interval in the mature oil to early wet-gas zones. However, the significantly higher reflectance of graptolites appears to suggest the sediments reached a higher level of maturation in the wet-gas to dry-gas generative zone.

Comparing the vitrinite-equivalent reflectance data against thermal maximum (T_{max}) data sourced from Rock-Eval pyrolysis provides a check for the reliability of the converted datasets and a more robust estimate of thermal maturity for potential petroleum source rocks in the Nambeet Formation. Vitrinite-equivalent T_{max} values ranged from TR_o = 0.7 to 1.0% suggesting maturity in the oil to early wet-gas generating zones. This agrees with the bitumen and zooclast data. Conodont material recovered from the Nambeet and Willara Formations have a colour alteration index (CAI) for conodonts of 1.5 – 2, in agreement with the TR_o data. Thermal alteration indices (TAI) from spore-pollen material in the Grant Group and Nambeet Formation indicate anomalously high maturities for both formations when compared to the other datasets.

KEYWORDS: bitumens, graptolites, thermal maturity, vitrinite reflectance

Introduction

Petroleum source-rock maturation is the continuous, irreversible evolution of organic matter to hydrocarbons (Barker, 1979). The main processes controlling thermal maturation are temperature and the amount of time the potential source rocks are exposed to various temperature ranges. The T_{max} temperature range where most oil generation occurs from petroleum source rocks is 435–470º C.

Analytical methods normally used to calculate thermal maturity of petroleum source rocks include vitrinite reflectance (VR), thermal alteration index (TAI), colour alteration index (CAI) for conodonts, and Rock-Eval (thermal maximum, T_{max}). However, the different methods can lead to erroneous or conflicting results, and use of VR depends on the source rocks containing vitrinite. Vitrinite is absent in sedimentary rocks deposited prior to the evolution of land plants. This means the thermal maturity of pre-Devonian source rocks must be determined by other methods.

Petroleum source rocks identified from the Ordovician upper Nambeet Formation were cored in petroleum well Olympic 1 (Figs 1, 2). The Nambeet Formation is subdivided into two distinct informal stratigraphic intervals: a lower sandstone unit and an upper shale unit (Fig. 3). A total of 312.92 m of core was obtained through this Lower Ordovician (Tremadocian to Floian) section, revealing organic-rich mudstone intervals in the upper Nambeet shale member (Fig. 3). Detailed information on the geological setting and the petroleum source-rock potential of the Nambeet Formation is given in Normore and Dent (2017).

The age of these rocks means they lack vitrinite and conventional VR methods for assessing thermal maturity are not available. However, the rocks contain bitumen and zooclasts, such as graptolites, and thermal maturity may be interpreted using alternative organic petrology methods.

In this Report, we examine methods for converting bitumen and zooclast reflectance to the vitrinite-equivalent reflectance to assess the thermal maturity of potential source rocks from the Lower Ordovician succession, Nambeet and Willara Formations, of the Broome Platform.

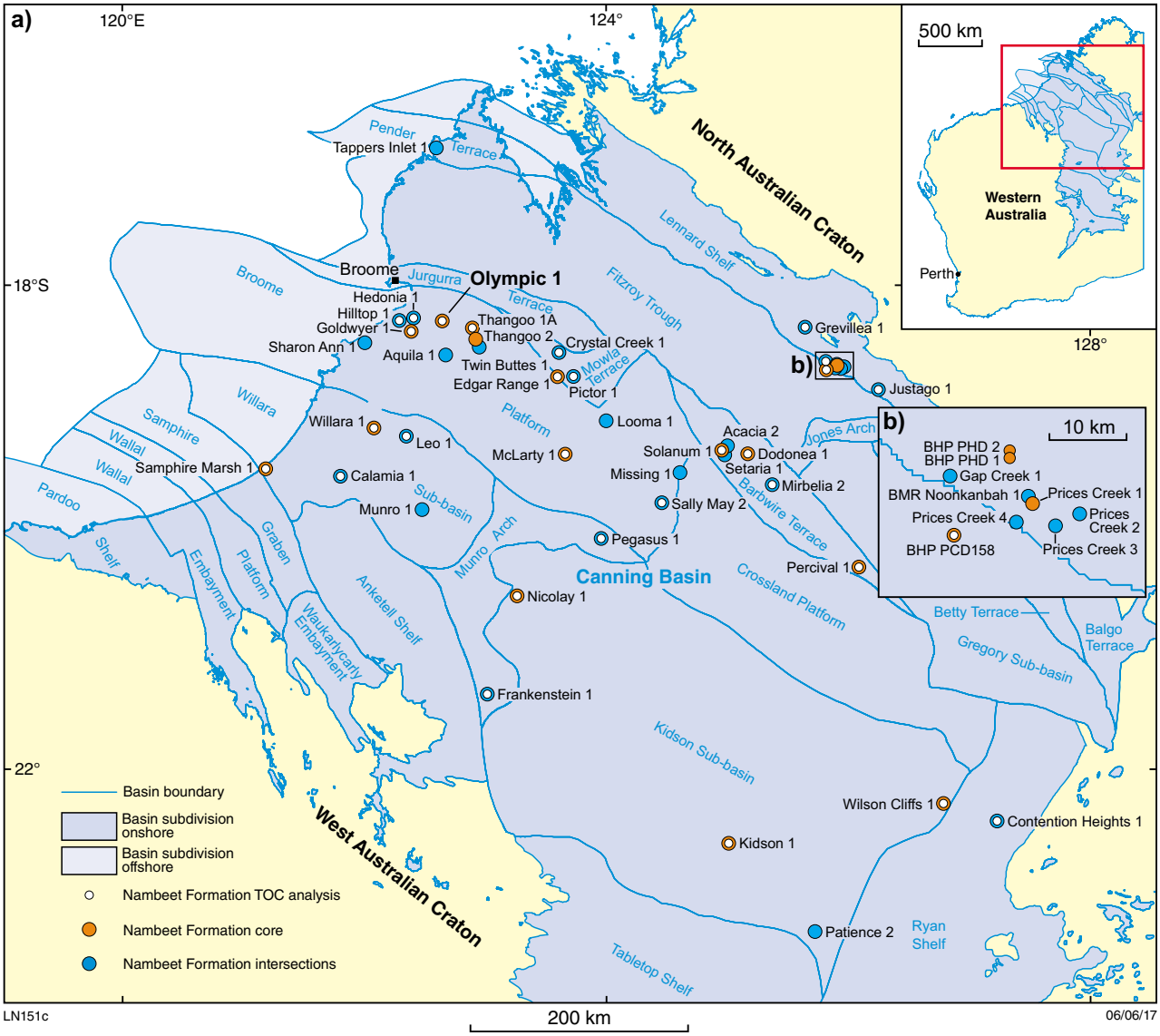

Figure 1. Tectonic subdivisions of the Canning Basin showing location of petroleum exploration well Olympic 1 and other wells that intersect the Nambeet Formation, wells where core was recovered, and wells for which organic geochemistry analysis was undertaken. Inset b) gives details of closely spaced wells in the northeast Canning Basin

These results were cross-checked against the estimated maturity using T_{max}, CAI and TAI values derived from Rock-Eval tests on samples from Olympic 1 to compare the robustness and validity of the results from the different data types.

Assessing thermal maturity

The potential for sedimentary rock to be a hydrocarbon source is defined by a number of geochemical factors. Thermal maturity is a key factor that determines the quantity and type of hydrocarbons generated: oil, wet gas or dry gas. Vitrinite reflectance is one of the main organic petrographic analyses used to quantify source-rock maturity (Dow, 1977; Hunt, 1996). However, the limitations of this method include:

- correct identification of the vitrinite maceral
- interpretation of the temperature range of the oil-generation window, which varies depending on the composition of the original kerogen (Tissot and Welte, 1978; Wilkins, 1999)
- the subjectivity of visually estimating reflectance depending on the skill and experience of the interpreter
- the absence of vitrinite in sedimentary rocks deposited prior to the existence of land plants, which did not evolve until the late Silurian (Petersen et al., 2013).

To assess the thermal maturity of the Lower Ordovician Nambeet Formation, we were required to use reflectance measured from other forms of organic material including zooclasts and graptolites (Cole, 1994; Petersen et al., 2013)

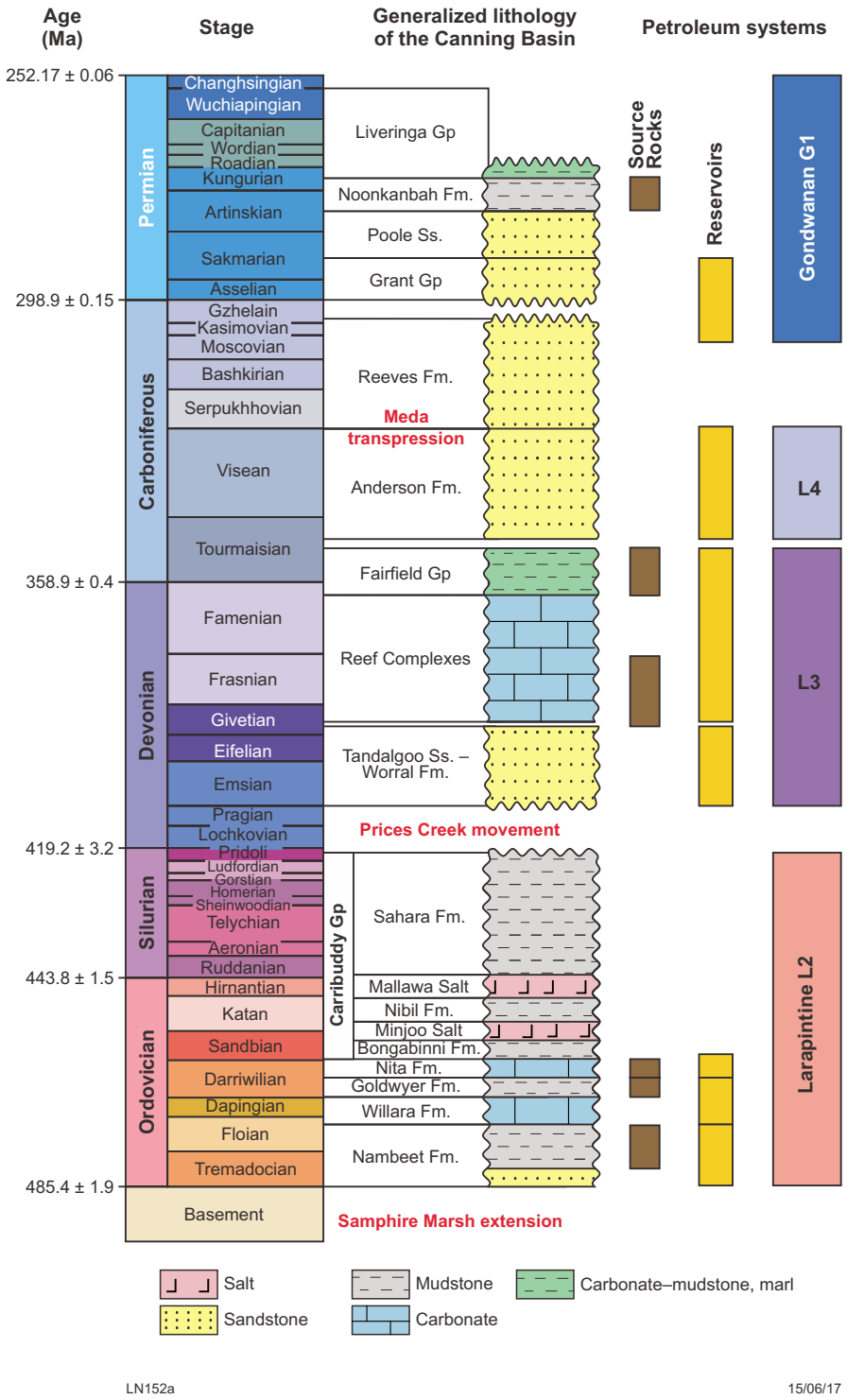

Figure 2. **Permian to Ordovician stratigraphy of the Canning Basin showing generalized lithology and the position of potential source rock and reservoir intervals, and petroleum systems. Modified after Ghori (2013); time scale after International Commission on Stratigraphy (2013)**

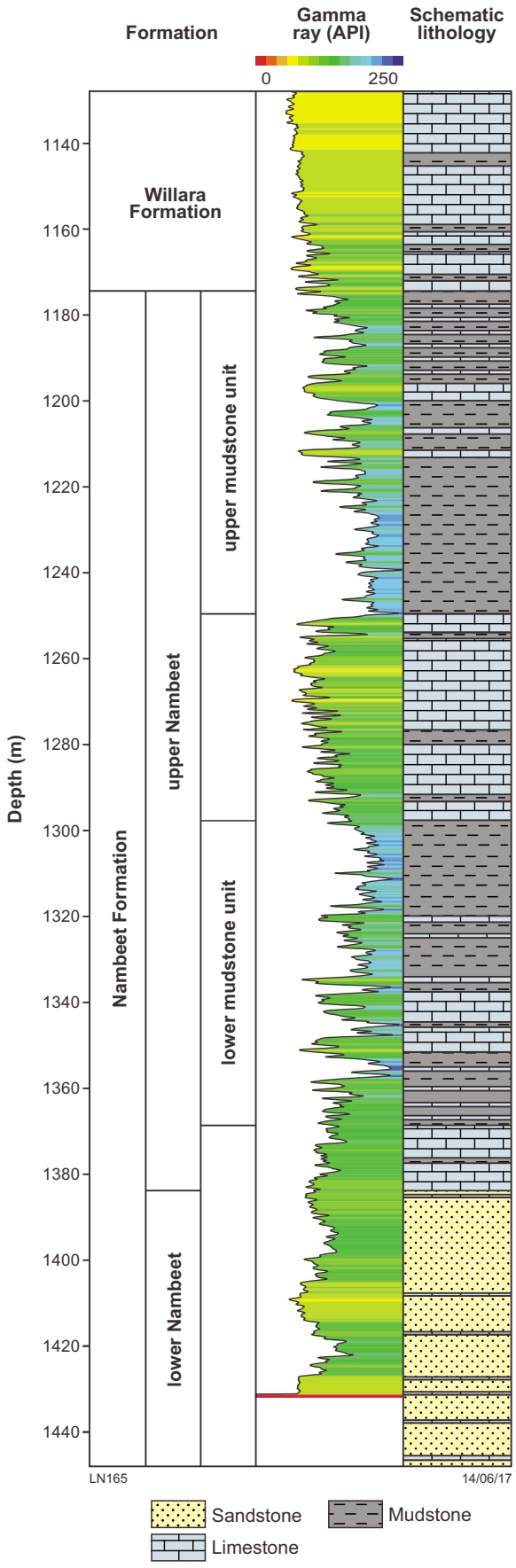

— and solid organic matter, i.e. bitumen (Jacob, 1989; Landis and Castaño, 1995; Schoenherr et al., 2007). These reflectance values were then converted to vitrinite-equivalent reflectance values. Determining thermal maturity from these converted equivalent values has varying levels of success.

Source maturity can also be interpreted using the T_{max} measurement from Rock-Eval pyrolysis, which provides a direct measure of kerogen conversion to petroleum, expressed as kerogen transformation (thermal maturity). The type of organic matter influences the T_{max} values, so this must be known when inferring thermal maturity (Espitalié et al., 1985; Wilkins, 1999; Ghori, 2013). T_{max} values may also have limited validity if two S_2 peaks have been recorded for the same sample (e.g. Schoenherr et al., 2007). It is common to compare vitrinite reflectance to T_{max} data to establish the robustness of both types of data.

Vitrinite reflectance analyses were performed on cuttings samples from Permian–Carboniferous and younger strata in the Olympic 1 well (Fig. 4a,b). One cuttings sample was also recovered from the Willara Formation. Vitrinite was not recorded in Nambeet or Willara Formation core or cuttings samples; however, bitumen (Fig. 4c,d), graptolites (Fig. 4e,f) and bioclasts (Fig. 4g,h) were present and their reflectance measured. The Nambeet Formation, the focus of this study and a potential source interval, is estimated to be of Lower to Middle Ordovician age based on biostratigraphy (Guppy and Orpik, 1950; McTavish, 1969; Nicol, 1993).

This investigation has three aims:

- determine the maturity of the Nambeet Formation in Olympic 1 by converting bitumen (B_{max}), graptolite (G_{max}) and bioclast (BC_{max}) reflectance data to vitrinite-equivalent reflectance values for bitumen (BR_o), graptolite (GR_o) and bioclast (BCR_o). Comparison of these vitrinite-equivalent values will determine if the results are robust and can be used as a reasonable estimate for thermal maturity
- compare BR_o, GR_o and BCR_o with the T_{max} values obtained throughout the cored interval in Olympic 1 to assess the reliability of the methodology for predicting the thermal maturity of the Nambeet Formation shales elsewhere in the Canning Basin
- compare maturity data from the Nambeet Formation intersected in other wells drilled in the Canning Basin to understand regional trends.

Figure 3. Stratigraphy of core (1128.0–1447.2 m) taken through the Willara and Nambeet Formations, Olympic 1, showing coloured gamma ray log and schematic lithology. The Nambeet Formation is informally divided into an upper mudstone-dominated unit and a lower sandstone unit. Two potential petroleum source intervals are identified in the upper Nambeet section; after Normore and Dent (2017)

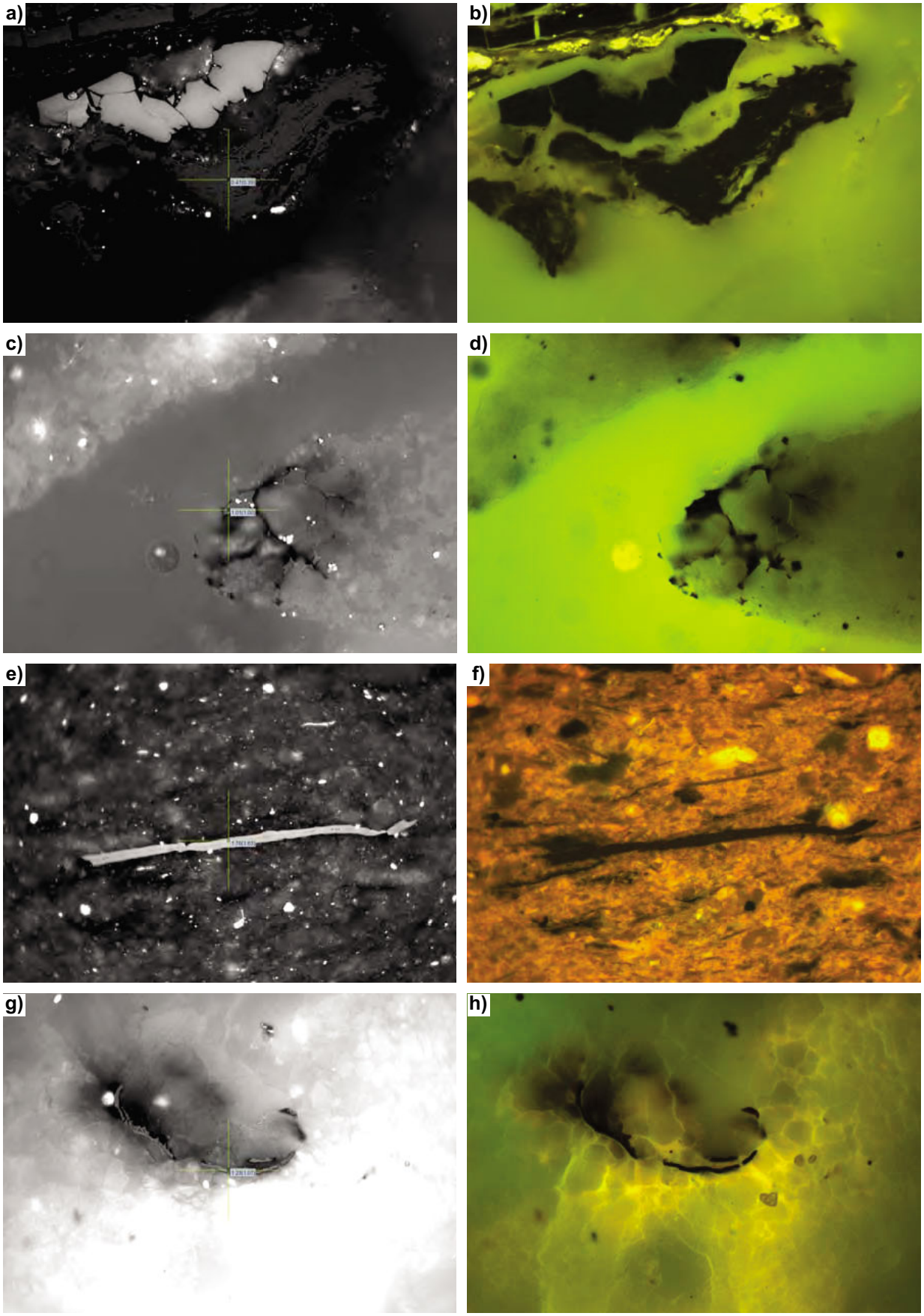

Figure 4. **Reflectance images for vitrinite and other organic components: a) vitrinite, reflected white light; b) vitrinite, fluorescence; c) bitumen, reflected white light; d) bitumen, fluorescence; e) graptolite, reflected white light; f) graptolite, fluorescence; g) bioclast, reflected white light; h) bioclast, fluorescence**

Reflectance standardization methodology

Bitumen reflectance standardization

The following section presents four methods for converting bitumen reflectance (B_{max}) values into vitrinite-equivalent reflectance (BR_o) values (Fig. 5) and outlines the parameters and assumptions of each method.

Jacob (1989)

Jacob (1989) derived the equation for bitumen reflectance values (BR_o) between <0.1% and ~3%:

$$BR_o = 0.618(B_{max}) + 0.4 \quad \text{(Eq. 1)}$$

Jacob (1989) produced the model to assess conventional hydrocarbon systems, and derived the equation from a case study using carbonate rocks which commonly act as reservoirs for migrated hydrocarbons. It is assumed in this equation that B_{max} is reflectance measured from migrated bitumen. Bitumen within the Nambeet Formation samples in Olympic 1 is probably in situ bitumen because, despite having variable carbonate content, the potential Nambeet Formation source rocks are predominantly clastic, and samples were mainly recovered from shale units. As a result, this method may be of limited relevance to bitumen samples from the Nambeet Formation.

Landis and Castaño (1995)

The Landis and Castaño (1995) equation was developed for values of BR_o <4 based on the observation that when BR_o >4, BR_o and B_{max} appear to be equal. The equation was derived from bitumen samples with BR_o in the range 0.5 – 5%:

$$BR_o = (B_{max} + 0.41)/1.09 \quad \text{(Eq. 2)}$$

This equation differs from that of Jacob (1989) because the parameters were derived using samples from low-permeability rocks — shales and siltstones — with the aim of measuring indigenous or in situ rather than migrated bitumen. They also noted that in closely spaced sandstone–shale pairs, both R_o and BR_o are more variable.

Schoenherr (2007)

Schoenherr et al. (2007) combined the datasets of both Jacob (1989) and Landis and Castaño (1995) to derive a new equation:

$$BR_o = (B_{max} + 0.2443)/1.0495 \quad \text{(Eq. 3)}$$

In their study, Schoenherr et al. (2007) observed that B_{max} values did not show a linear depth trend. This was attributed to two generations of reservoir bitumen, an interpretation validated by the microstructure of the bitumen. Schoenherr et al. (2007) also analysed T_{max} and interpreted it to have limited validity and suggested there are two S_2 peaks, with one at low temperatures.

Bertrand and Malo (2012)

Bertrand and Malo (2012) took a different approach and used two different equations for different lithologies:

$$BR_o = 0.8113(B_{max}^{1.2438}) \quad \text{(shale–marl)} \quad \text{(Eq. 4)}$$

$$BR_o = 1.2503(B_{max}^{0.904}) \quad \text{(limestone)} \quad \text{(Eq. 5)}$$

In both equations the bitumen is assumed to be migrated bitumen. Bertrand and Malo (2012) also indicated that values are not finite; rather, a raw bitumen reflectance value will translate to a range of possible BR_o equivalents.

Graptolite and bioclast reflectance standardization

The method for converting graptolite reflectance to a vitrinite-equivalent reflectance is more challenging than for bitumen. There is general agreement that graptolites are more reflective than vitrinite at equivalent thermal maturities (Link et al., 1990; Cole, 1994; Petersen et al., 2013). The majority of equations derived for converting graptolite reflectance to its vitrinite equivalent also include allowance for 'vitrinite-like particles' (VLP), often assumed to be graptolite fragments but which cannot be definitively identified as graptolites by morphology (Xianming et al., 2000; Petersen et al., 2013).

The following section presents three methods for converting graptolite reflectance (G_{max}) values into normalized vitrinite-equivalent reflectance (GR_o) values (Fig. 6a) and outlines the parameters and assumptions of each method.

Bertrand and Malo (2012)

Bertrand and Malo (2012) converted G_{max} according to the expression:

$$GR_o = 0.9376(G_{max}) + 0.0278 \quad \text{(Eq. 6)}$$

This equation is based on the equations derived by Bertrand (1990) and later verified by Bertrand (1993). Bertrand (1990) compared graptolite reflectance specifically to the vitrinite form telinite and derived the relationship between the two indirectly by identifying the relationship between vitrinite and chitonozoans, and then the relationship between chitonozoans and graptolites. The resulting equation indicated the reflectance of graptolites was slightly lower than that of telinite at the same thermal maturity (Bertrand, 1990, 1993). However, the equations from Bertrand (1990, 1993) were modified by Bertrand and Malo (2012) who determined that the reflectance of graptolites was slightly higher than that of telinite at the same thermal maturity. This is consistent with results from Cole (1994) and Petersen et al. (2013).

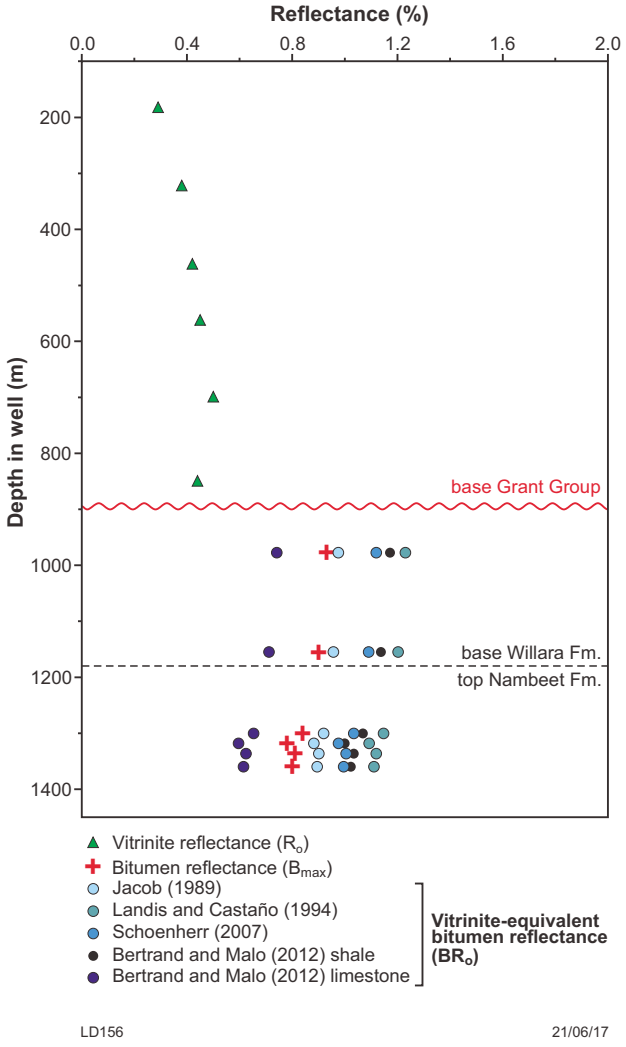

Figure 5. Normalized vitrinite-equivalent reflectance from bitumen in Olympic 1. Raw bitumen reflectance (B_{max}) values transformed into vitrinite-equivalent reflectance (BR_o) values according to equations by Jacob (1989), Landis and Castaño (1995), Schoenherr et al. (2007), and Bertrand and Malo (2012). All calculated BR_o values are greater than actual vitrinite reflectance values (R_o) from higher in the well, but BR_o decreases with depth

Cole (1994)

Cole (1994) derived the following transformations:

$$1.1\%\ G_{max} = 0.9\%\ GR_o \quad \text{(anoxic)} \qquad \text{(Eq. 7)}$$

$$1.1\%\ G_{max} = 0.7\%\ GR_o \quad \text{(dysoxic)} \qquad \text{(Eq. 8)}$$

Cole (1994) determined that environmental factors, specifically the oxygen levels in the water column and sediments at the time of deposition, significantly influence the reflectivity of graptolite fragments. More oxygen-rich (oxic) conditions produce a higher reflectivity than oxygen depleted or anoxic conditions, and the reflectance of graptolites deposited in oxic conditions records the greatest difference between true and apparent maturity. The results of Cole (1994) suggest that in dysoxic conditions GR_o is 35% lower than G_{max} and in anoxic sediments GR_o is 20% lower than G_{max}. The sediments of the Nambeet Formation are interpreted as anoxic and the data have therefore been transformed according to the 'anoxic' equation (Eq. 7) for the purpose of this study.

Petersen et al. (2013)

Petersen et al. (2013) developed the following equation to convert G_{max} to GR_o:

$$GR_o = 0.73\ G_{(max\ +\ vitrinite\text{-}like)\ low} + 0.16 \qquad \text{(Eq. 9)}$$

This equation was developed based on datasets that showed equal reflectance of graptolites and VLP. Petersen et al. (2013) assumed the VLP were graptolite fragments, based on a linear relationship and strong positive correlation between the reflectance of the positively identified graptolite fragments and the VLP (Fig. 7a).

Both graptolite fragments and graptolite periderms are identified in Olympic 1, but the reflectance values were recorded separately and the graptolite periderm reflectance data referred to as Bioclast 1. Applying equation 9 to Bioclast 1 data presumes the bioclasts are equivalent to material Petersen et al. (2013) identified as VLP. However, the crossplot of graptolite and Bioclast 1 datasets from Olympic 1 shows no correlation between these components (Fig. 7b). Given this, it appears the assumption that the bioclasts are equivalent to VLP may not be justified, and it is more appropriate to treat the two datasets separately.

The reflectance values for the Bioclast 1 data also include values for what may be algal matter. The lack of correlation between two sets of graptolite data suggests some level of interference, potentially by the algal matter included in the readings. For this reason the data are transformed using the same equation but treated separately. Raw Bioclast 1 reflectance data is designated as BC_{max} and vitrinite-equivalent reflectance values are referred to as BCR_o. The reflectance of graptolite fragments is referred to as Graptolite data, raw reflectance data is designated as G_{max}, and vitrinite-equivalent reflectance values are referred to as GR_o:

$$GR_o = 0.73\ G_{(max)\ low} + 0.16 \qquad \text{(Eq. 10)}$$

$$BCR_o = 0.73\ BC_{(max)\ low} + 0.16 \qquad \text{(Eq. 11)}$$

Results

Vitrinite-equivalent bitumen reflectance (BR_o)

The mean bitumen reflectance values (B_{max}) show an unexpected trend of decreasing reflectance with depth with a correlation coefficient of 0.87 (Fig. 5). Standard deviation ranges from 0.038 to 0.145 and number of counts per sample is variable (Table 1). When transformed

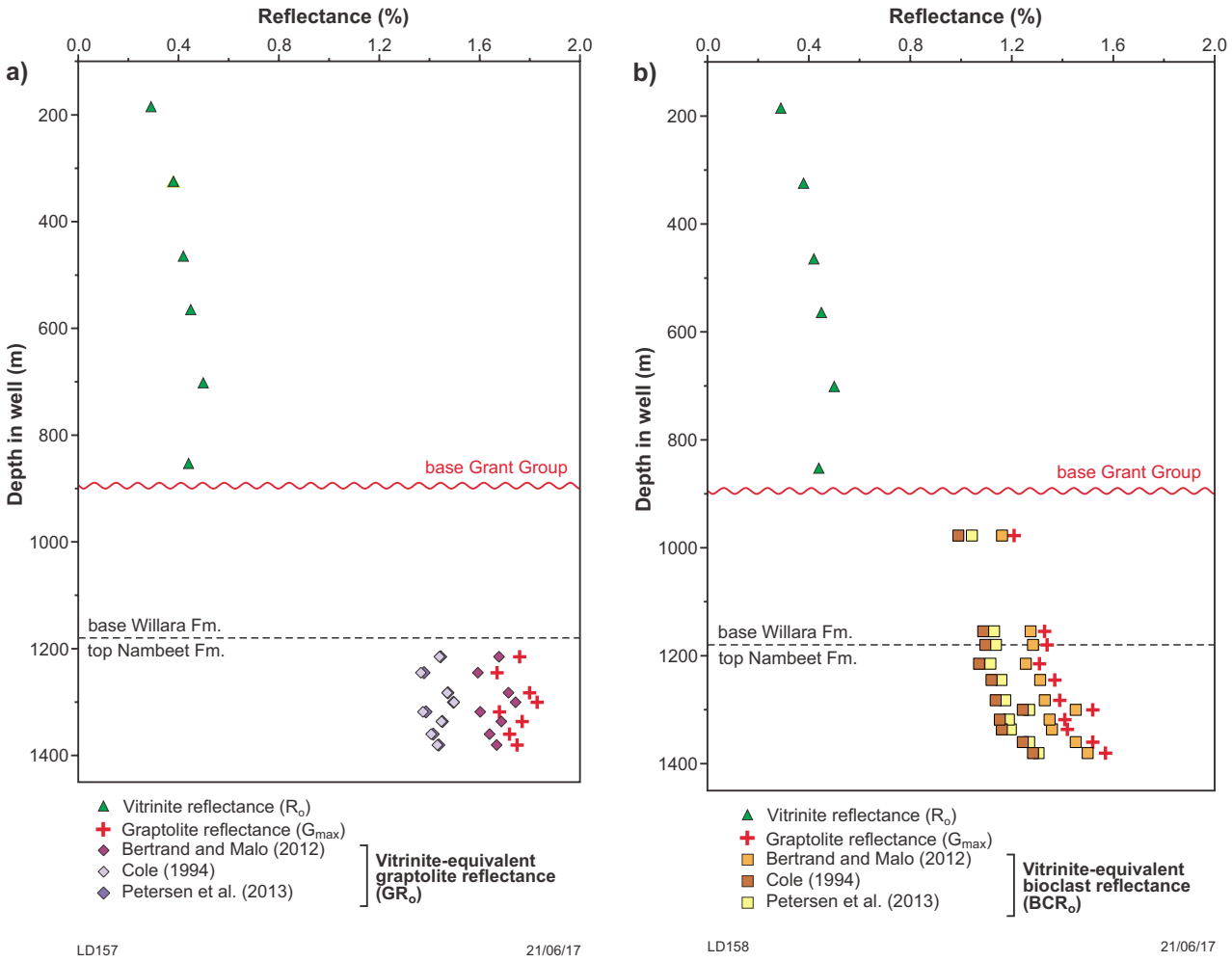

Figure 6. **Vitrinite-equivalent reflectance derived from graptolite and bioclast reflectance in Olympic 1: a) graptolite reflectance (G_{max}) transformed into vitrinite-equivalent reflectance (GR_o) values according to three equations by Bertrand and Malo (2012), Cole (1994), and Petersen et al. (2013). All GR_o values are greater than actual vitrinite reflectance values (R_o) from higher in the well, but there is no correlation of graptolite reflectance with depth; b) bioclast reflectance (BC_{max}) transformed into vitrinite-equivalent reflectance (BCR_o) values according to three equations by Bertrand and Malo (2012), Cole (1994), and Petersen et al. (2013). All BCR_o values are greater than actual vitrinite reflectance values (R_o) from higher in the well. In this case, there is a good correlation of increasing bioclast reflectance with increasing depth**

according to equations 1–5 (Table 2), the dataset showed significant variation (Fig. 5). Interestingly the Bertrand and Malo (2012) transformation for shales (Eq. 4) plotted the lowest BR_o values and the Landis and Castaño (1995) transformation for siltstone and mudstone (Eq. 2) plotted the highest BR_o values (Fig. 5). There is significant overlap in the range of values between data transformed according to the Jacob (1989), Landis and Castaño (1995), Schoenherr et al. (2007), and Bertrand and Malo (2012) limestone equations, with the exception of the lowest Bertrand and Malo (2012) shale transformation dataset.

Data pitfalls

The inability to define a bitumen-to-vitrinite reflectance equivalent conversion that is globally applicable is a repeating theme in the literature. The conversion of bitumen to vitrinite-equivalent reflectance is influenced by numerous factors making it difficult to agree on a general rule. The three main influencing factors cited are:

- differences in lithology (Bertrand, 1990; Landis and Castaño, 1995; Bertrand and Malo, 2012)
- bitumen type; migrated vs in situ or matrix (Jacob, 1989; Gentzis and Goodarzi, 1990; Landis and Castaño, 1995; Ardakani et al., 2014)
- the relationship and variation of bitumen reflectance at different thermal maturities (Jacob, 1989; Bertrand, 1990; Landis and Castaño, 1995; Bertrand and Malo, 2001).

Bitumen is typically less reflective than vitrinite at equivalent thermal maturities. When the raw bitumen reflectance data was converted according to the

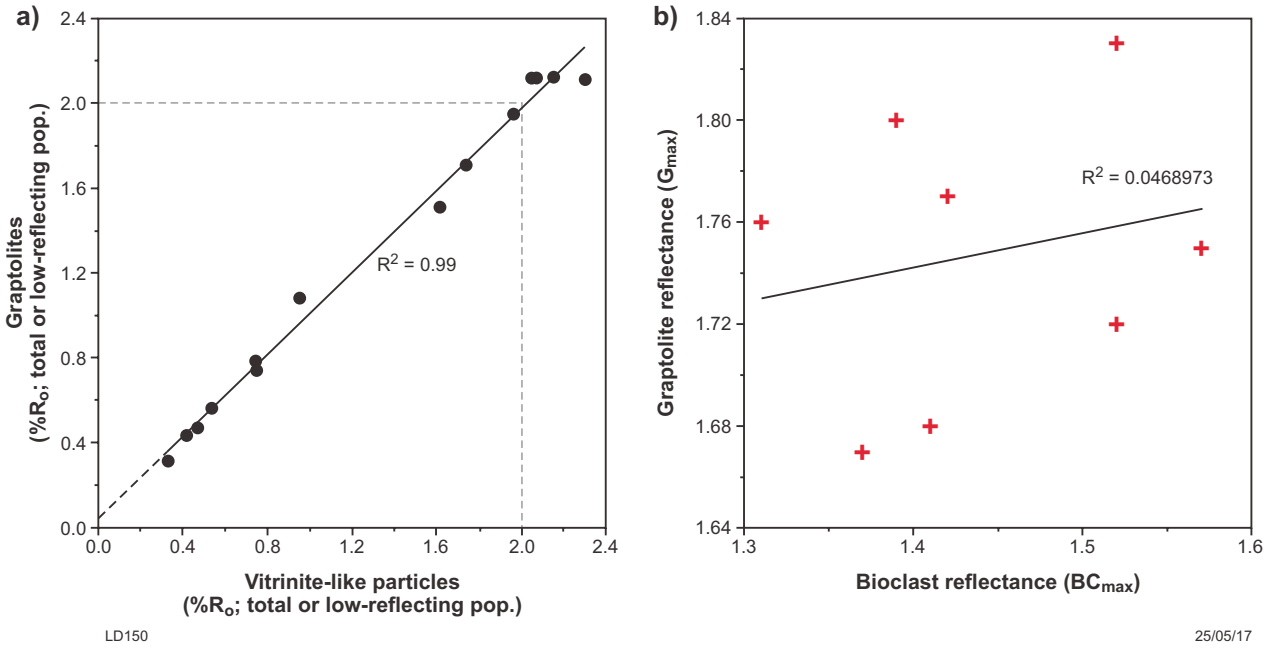

Figure 7. Correlation of vitrinite-like particle (VLP) reflectance, bioclast (BC_{max}) reflectance, and graptolite reflectance: a) figure adapted from Petersen et al. (2013) illustrating a strong linear relationship between VLP and graptolite reflectance values, suggesting that VLP are also graptolite fragments; b) correlation of bioclast BC_{max} and graptolite G_{max} reflectance from Olympic 1. Raw reflectance values of the Bioclast 1 dataset and the graptolite fragments recovered from equivalent depths show no significant correlation $R^2 = 0.047$

equations 1–5 above, four equations reflected this relationship; the exception is the Bertrand and Malo (2012) equation for bitumen conversion in shale lithologies (Eq. 4). The BR_o values produced from this equation had the largest difference compared to BR_o values derived from Landis and Castaño (1995); their method was also developed for conversion of bitumen in shale lithologies. Based on these differences, the results derived using the Bertrand and Malo (2012) transformation for shale lithologies are treated with low confidence.

Bertrand and Malo (2012) reported that, when transformed using equation 4, a single B_{max} value will result in a range of values, within which the value generated by this equation is the maximum in the range; e.g. a B_{max} of 1% will convert to a value within the range BR_o 0.95 to 1.25% and the equation will determine a value of BR_o 1.25%. When the Olympic 1 data are converted using this equation, the resulting range of values overlaps with BR_o values converted according to Jacob (1989) and Schoenherr et al. (2007). Good confidence is attributed to the outcome of all three methods and the combined results supply an estimated range for BR_o values in the Olympic 1 well.

Discussion of bitumen results

Variation in bitumen reflectance

There is a distinct increase in reflectance values between the vitrinite reflectance (R_o) values in the younger Grant Group sediments that overlie the Nambeet Formation and the bitumen reflectance (BR_o) values within the Nambeet Formation (Fig. 5). This increase indicates the deeper sediments are more thermally mature, as expected. The abruptness of the increase can be attributed to the presence of a major regional unconformity at approximately 898 m depth where late Carboniferous – early Permian sedimentary rocks of the Grant Group overlie the Ordovician sedimentary rocks. The unconformity represents an age gap of over 140 million years. Although the thickness of missing section has not been estimated in this well, thick Middle Ordovician strata, including the Willara, Goldwyer and Nita Formations are present in nearby wells. Petroleum exploration well Aquila 1, only 31 km to the south, has 882 m of post-Nambeet Ordovician sedimentary rocks (Karajas and Taylor, 1983), compared to 282 m in Olympic 1. This suggests substantial erosion and potentially much deeper burial of the Ordovician strata, including the Nambeet Formation, in Olympic 1 than the preserved thickness of strata would suggest.

Within the Ordovician strata, the BR_o dataset shows a decrease in reflectance with depth, between the Willara and Nambeet Formations, which is unusual and unexpected (Fig. 5). There are two possible reasons for this trend: firstly, the change in lithology downhole from carbonate-dominated facies to shale-dominated facies; secondly, the presence of multiple hydrocarbon phases, either in situ and migrated or multiple migrated phases.

Table 1. Vitrinite reflectance (R_o) and bitumen reflectance (B_{max}) values for core and cuttings from the Olympic 1 well. R_o and B_{max} at each sample depth are means of all maximum vitrinite and bitumen reflectance readings, respectively; range is lowest and highest R_o or B_{max} of the population considered to represent the first generation. Abbreviations: SD, standard deviation; N, number of fields measured (actual number of measurements = 2N because two maximum values were recorded for each field)

Depth (m)	*R_o*	*B_{max}*	*Range*	*SD*	*N*
185	0.29	–	0.24 – 0.37	0.041	7
325	0.38	–	0.28 – 0.45	0.036	25
465	0.42	–	0.32 – 0.54	0.058	25
565	0.45	–	0.35 – 0.61	0.07	19
701.5	0.5	–	0.43 –0.62	0.074	4
852.5	0.44	–	0.39 – 0.49	0.041	3
977.5	–	0.93	0.75 – 1.05	0.093	9
1154.87	–	0.9	0.66 – 0.109	0.145	7
1300.35	–	0.84	0.75 – 0.92	0.056	6
1318.38	–	0.78	0.69 – 0.87	0.09	2
1336.42	–	0.81	0.68 – 0.97	0.108	7
1359.97	–	0.8	0.75 – 0.89	0.038	14

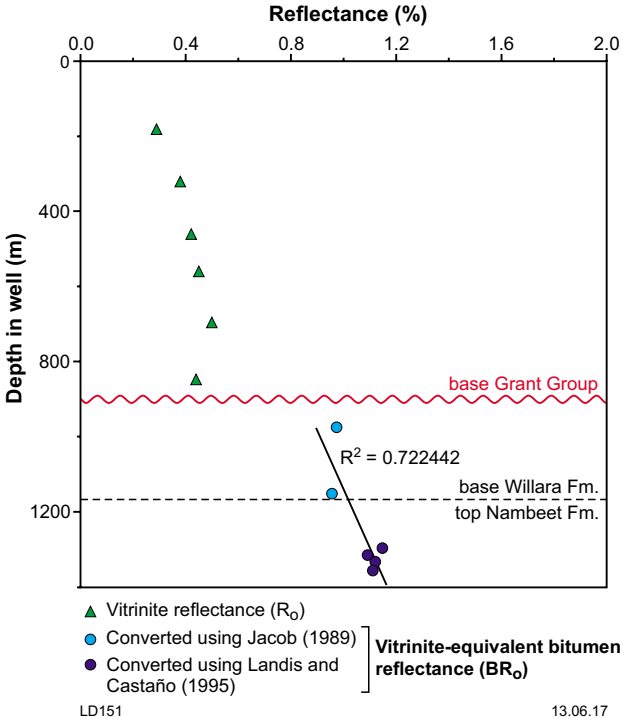

Figure 8. Normalized vitrinite-equivalent reflectance derived from bitumen reflectance in Olympic 1. Raw bitumen reflectance values (B_{max}) are transformed into the equivalent vitrinite reflectance values (BR_o) according to lithology. The top two Willara Formation carbonate samples are transformed according to Jacob (1989), and the deeper Nambeet Formation mudstone samples transformed according to Landis and Castaño (1995)

Bitumen reflectance (B_{max}) is influenced by lithology (e.g. Bertrand, 1990). To account for this, different conversion equations were developed for different lithologies (Jacob, 1989; Landis and Castaño, 1995; Bertrand and Malo, 2012). The two shallowest BR_o data points from Olympic 1 are from the carbonate-dominated Willara Formation and the lower four samples are from the shale-dominated Nambeet Formation. If the Willara Formation samples are converted according to carbonate-specific equations (Eq. 1; Jacob, 1989) and the Nambeet Formation samples are converted with shale-specific equations (Eq. 2; Landis and Castaño, 1995), a standard trend of increasing reflectance with depth results (Fig. 8).

However, a decreasing reflectance with depth trend could also be caused by migration of hydrocarbons in the system if more mature bitumen migrated upwards into less mature sediments. Oil shows are observed within some sandstone lithofacies in the core through the Nambeet Formation and small oil bleeds are present in carbonate lithofacies of the Willara Formation and are interpreted as migrated hydrocarbons. The presence of two different generations of bitumen, migrated bitumen in the Willara Formation from a more thermally mature source, and matrix bitumen in the upper Nambeet shale member, could explain the inverse thermal maturity trend. If so, the reflectance values obtained for shallowest samples from the Willara Formation would not reflect the true maturity of the host rock. In contrast, the calculated maturity using the matrix bitumen of the Nambeet Formation would be more reliable, and more likely reflect the maturity of the host rock. Therefore, these matrix bitumen results can be interpreted with greater confidence. Other factors that should be considered are the variations in bitumen reflectance that have been recorded depending on maturation and migration stage — pre-oil and post-oil, in situ versus migrated — and particle texture (Gentzis and Goodarzi, 1990; Sanei et al., 2015; Hackley and Cardott, 2016).

The variability in the BR_o values may also be attributed to the existence of two migrated bitumen phases. Schoenherr et al. (2007) interpreted this phenomenon from distinct bimodal distributions observed in their bitumen reflectance data (Fig. 9a,b) and differences in the microstructure of the bitumen. Confident identification of a bimodal distribution in the reflectance data from Olympic 1 would require a greater number of measurements (Fig. 9c–f).

Vitrinite-equivalent graptolite (GR_o) and bioclast (BCR_o) reflectance

The plot of graptolite reflectance displays moderate scatter in the data and no depth trend over an interval of approximately 165 m (1215–1380 m; Fig. 6a, Table 3).

Table 2. Bitumen reflectance (B_{max}) values for samples from Olympic 1 converted to vitrinite-equivalent reflectance values (BR_o) using four different equations; see text for details. Abbreviations: Sh, shale; Ls, limestone

		Vitrinite-equivalent reflectance (BR_o)				
Depth (m)	*Bitumen reflectance (B_{max})*	*Jacob (1989)*	*Landis and Castaño (1995)*	*Schoenherr et al. (2007)*	*Bertrand and Malo (2012) Sh*	*Bertrand and Malo (2012) Ls*
977.5	0.93	0.975	1.229	1.119	0.741	1.170908117
1154.87	0.9	0.956	1.202	1.09	0.712	1.136709422
1300.35	0.84	0.919	1.1468	1.033	0.653	1.067978982
1318.38	0.78	0.882	1.0917	0.976	0.596	0.998775204
1336.42	0.81	0.901	1.119	1.005	0.624	1.033438622
1359.97	0.8	0.894	1.11	0.995	0.615	1.021898071

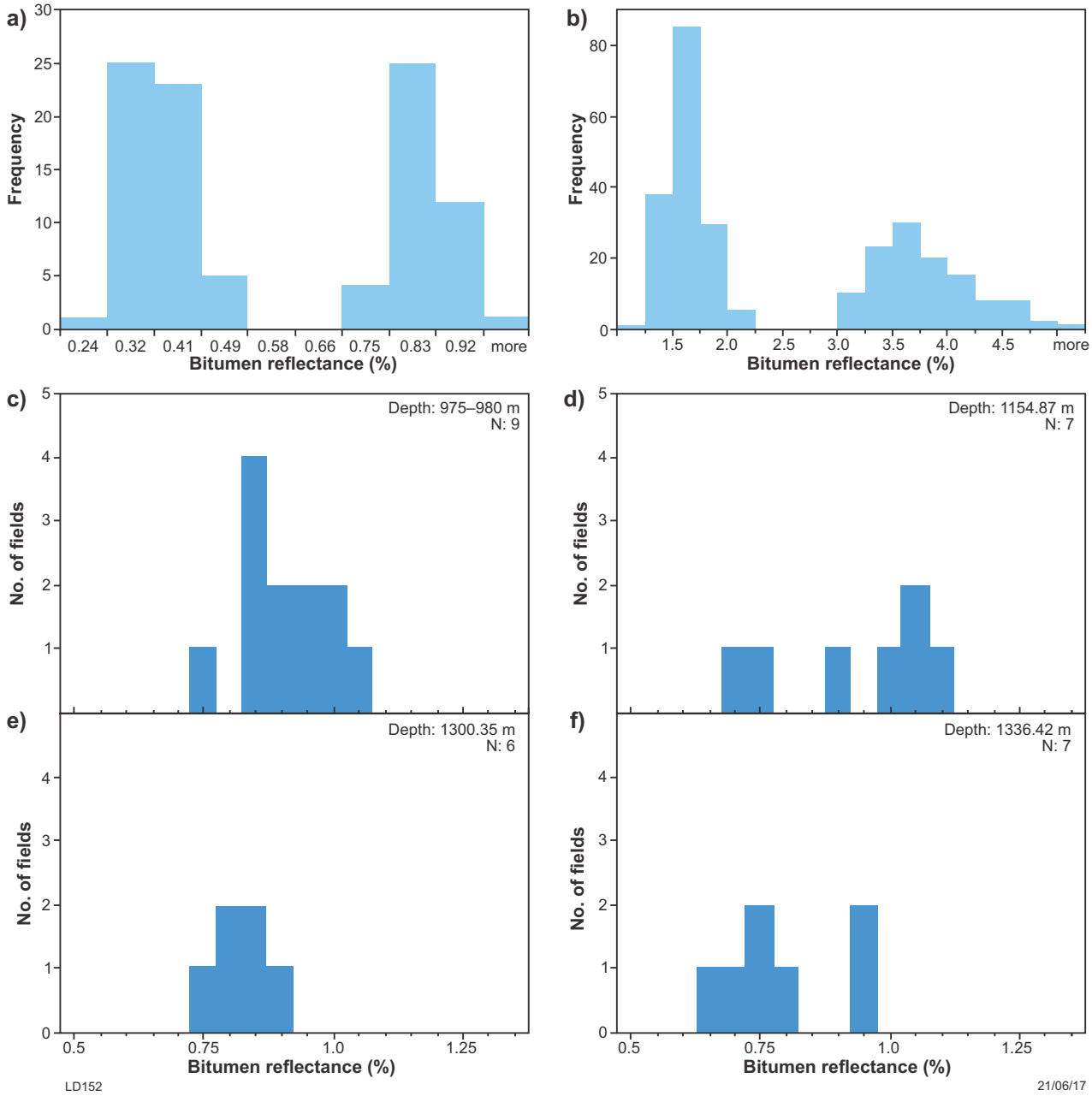

Figure 9. Bitumen reflectance distributions: a, b) bimodal bitumen reflectance distributions presented by Schoenherr et al. (2007) to infer the presence of two phases of migrated bitumen; c–f) bitumen reflectance (B_{max}) distributions from a selection of Olympic 1 samples showing possible unimodal distributions

Table 3. Graptolite and bioclast reflectance values for core and cuttings from the Olympic 1 well. G_{max} and BC_{max} are the means of all maximum graptolite and bioclast reflectance readings, respectively; range is the lowest and highest G_{max} and BC_{max} of the population considered to represent the first generation. Abbreviations: SD, standard deviation; N, number of fields measured (actual number of measurements = 2N because 2 maximum values were recorded for each field)

	Graptolite reflectance				*Bioclast reflectance*			
Depth (m)	*G_{max}*	*Range*	*SD*	*N*	*BC_{max}*	*Range*	*SD*	*N*
975–980					1.21	1.15 – 1.24	0.04	3
1154.87					1.33	1.13 – 1.65	0.138	30
1180.15					1.34	1.21 – 1.52	0.083	30
1215.02	1.76	-	-	1	1.31	1.09 – 1.55	0.116	30
1245.07	1.67	-	-	1	1.37	1.14 – 1.63	0.117	30
1282.74	1.8	-	-	1	1.39	1.14 – 1.72	0.138	30
1300.35	1.83	1.70 – 2.03	0.087	11	1.52	1.21 – 1.72	0.122	30
1318.38	1.68	1.55 – 1.84	0.08	20	1.41	1.18 – 1.60	0.106	30
1336.42	1.77	1.63 – 1.95	0.1	6	1.42	1.22 – 1.65	0.108	30
1359.97	1.72	1.52 – 2.02	0.137	11	1.52	1.24 – 1.66	0.101	30
1380.38	1.75	1.65 – 1.85	0.1	2	1.57	1.35 – 1.74	0.102	30

When transformed according to Cole (1994) and Petersen et al. (2013), the data plot in the range GR_o ~1.38 – 1.5% and there is a very narrow difference of only 0.03% between the results of the two methods (Table 4). When transformed according to Bertrand and Malo (2012), the resulting calculated reflectance plots higher than the other two methods with predicted maturity ranging between GR_o 1.59 to 1.74%.

Graptolite periderms and possible coalified filamentous blue-green algae (CFA) are present together in most samples which are referred to here as Bioclast 1 data (Table 5). Bioclast 1 reflectance values were converted using graptolite-equivalent equations. Because graptolites are not identified in the sample from 1380.38 m, this data point was omitted. Bioclast 1 samples showed a trend of increasing reflectance with increasing depth (Fig. 6b). The calculated reflectance values range between BCR_o 0.99 to 1.3 % when transformed according to equation 7 and equation 9 (Fig. 6b). Values transformed using equation 6 plot at much higher reflectance between 1.16 and 1.49%.

Both Graptolite and Bioclast 1 assemblages show predominantly unimodal distributions with a minor to moderate overlap between the assemblages (Fig. 10). Petersen et al. (2013) interpreted significant overlap between VLP and graptolite reflectance as evidence to suggest the two were the same. The clearly separate distributions in the Olympic 1 dataset reaffirm that the bioclast and graptolite datasets should not be combined.

Discussion of zooclast results

Variation in graptolite and bioclast reflectance

There is a clear relationship indicating that graptolites are more reflective than vitrinite at equivalent thermal maturities from all three conversion methods for graptolites and bioclasts. Typically a trend in the graptolite data, such that reflectance increases with depth, would be expected. The absence of this trend (Fig. 6a), and the lack of correlation between the graptolite and bioclast data (Fig. 7b), is unexpected.

Given the bioclast data in part comprises graptolite matter, the reflectance of the two datasets would be expected to correlate (Petersen et al., 2013). Graptolite structure can influence reflectivity (Link et al., 1990) and the differentiation between graptolite fragments and periderms (classified as Bioclast 1) may be related to preservation of different components of the original graptolite skeleton and result in variation in reflectivity.

A plot of the Bioclast 1 reflectance data against depth demonstrates a normal maturity trend of increasing reflectivity with depth. The graptolite fragment reflectance data is scattered and has no trend with depth and therefore low confidence is given to its reliability as a maturity indicator in Olympic 1. To determine if the graptolite reflectance is truly random, it was plotted against the interpreted in situ bitumen reflectance values in the upper Nambeet shale member. Interestingly, a strong positive linear trend is observed between the bitumen (B_{max}) and graptolite reflectance (G_{max}) (Fig. 11). The four samples that contain both bitumen and graptolites have a correlation coefficient of $R^2 = 0.9752$ and good sample counts. This suggests that the scatter in the graptolite data is not random and increases the confidence of this result.

The strong G_{max} to B_{max} correlation implies that the Nambeet Formation bitumen and graptolite fragments are influenced by a common factor that has insignificant influence on the Bioclast 1 data. Lithology is known to influence graptolite reflectance because samples recovered from limestones have a lower reflectance than those embedded within shales (Link et al., 1990). In the Olympic 1 cored section, samples were commonly taken across thinly interbedded shale–carbonate sections.

Table 4. Graptolite reflectance (G_{max}) values converted to vitrinite-equivalent reflectance values (GR_o) using three different equations; see text for details

		Vitrinite-equivalent reflectance (GR_o)		
Depth (m)	*Graptolite reflectance (G_{max})*	*Bertrand and Malo (2012)*	*Cole (1994)*	*Petersen et al. (2013)*
1215.02	1.76	1.678	1.44	1.445
1245.07	1.67	1.594	1.366	1.379
1282.74	1.8	1.715	1.473	1.474
1300.35	1.83	1.744	1.497	1.496
1318.38	1.68	1.603	1.375	1.386
1336.42	1.77	1.687	1.448	1.452
1359.97	1.72	1.64	1.407	1.416
1380.38	1.75	1.669	1.432	1.438

Table 5. Bioclast reflectance (BC_{max}) values, ranges of values, and components. Symbols: X indicates the presence of a component; * denotes possible presence of graptolite periderms; CFA, coalified filamentous blue-green algae

	Bioclast reflectance (BC_{max})		*Bioclast 1 components*	
Depth (m)	*Mean maximum*	*Range*	*Graptolite periderms*	*Possible CFA*
975–980	1.21	1.15 – 1.24	X*	
1154.87	1.33	1.13 – 1.65	X*	X
1180.15	1.34	1.21 – 1.52	X	X
1215.02	1.31	1.09 – 1.55	X	X
1245.07	1.37	1.14 – 1.63	X	X
1282.74	1.39	1.14 – 1.72	X	X
1300.35	1.52	1.21 – 1.72	X	X
1318.38	1.41	1.18 – 1.60	X*	X
1336.42	1.42	1.22 – 1.65	X*	X
1359.97	1.52	1.24 – 1.66	X*	X
1380.38	1.57	1.35 – 1.74		X

More frequent and targeted sampling would be required to determine the influence of lithology on the graptolite fragments in this well.

Cole (1994) noted that graptolite reflectance is strongly influenced by the oxygen levels at the time of deposition. It is possible, given the two different types of graptolite data — the fragments comprising the G_{max} dataset and the periderms comprising the BC_{max} data — that one group is allochthonous. Transportation of the graptolite fragments from more oxygenated depositional settings would produce a higher raw reflectance than that produced by the autochthonous graptolites in the BC_{max} data.

Estimate of thermal maturity

As expected, all converted reflectance values from the Ordovician are higher than vitrinite reflectance values from the Permian interval in the well (Fig. 12). Based on the combination of the BR_o, GR_o and BCR_o data, the thermal maturity of the upper Nambeet shale member is calculated to be equivalent to a vitrinite reflectance range of aproximately 0.9 – 1.74% (Fig. 12). According to the correlation of Hartkopf-Fröder et al. (2015), this equates to thermal maturity in the peak oil to peak wet-gas generation window. However, this range is too broad over a relatively thin interval to be valid. The ranges estimated from each of the different data types are not consistent with each other, and the higher reflectance values in the range are heavily skewed by the graptolite data (Fig. 12). In order to tighten the range of the estimated thermal maturity, R_o values were compared to T_{max} measurements.

Calculation of thermal maturity from T_{max}

T_{max} is the temperature of maximum hydrocarbon generation during Rock-Eval pyrolysis. Typically, T_{max} is plotted against production index (PI) to: 1) differentiate between mature, immature or contaminated samples;

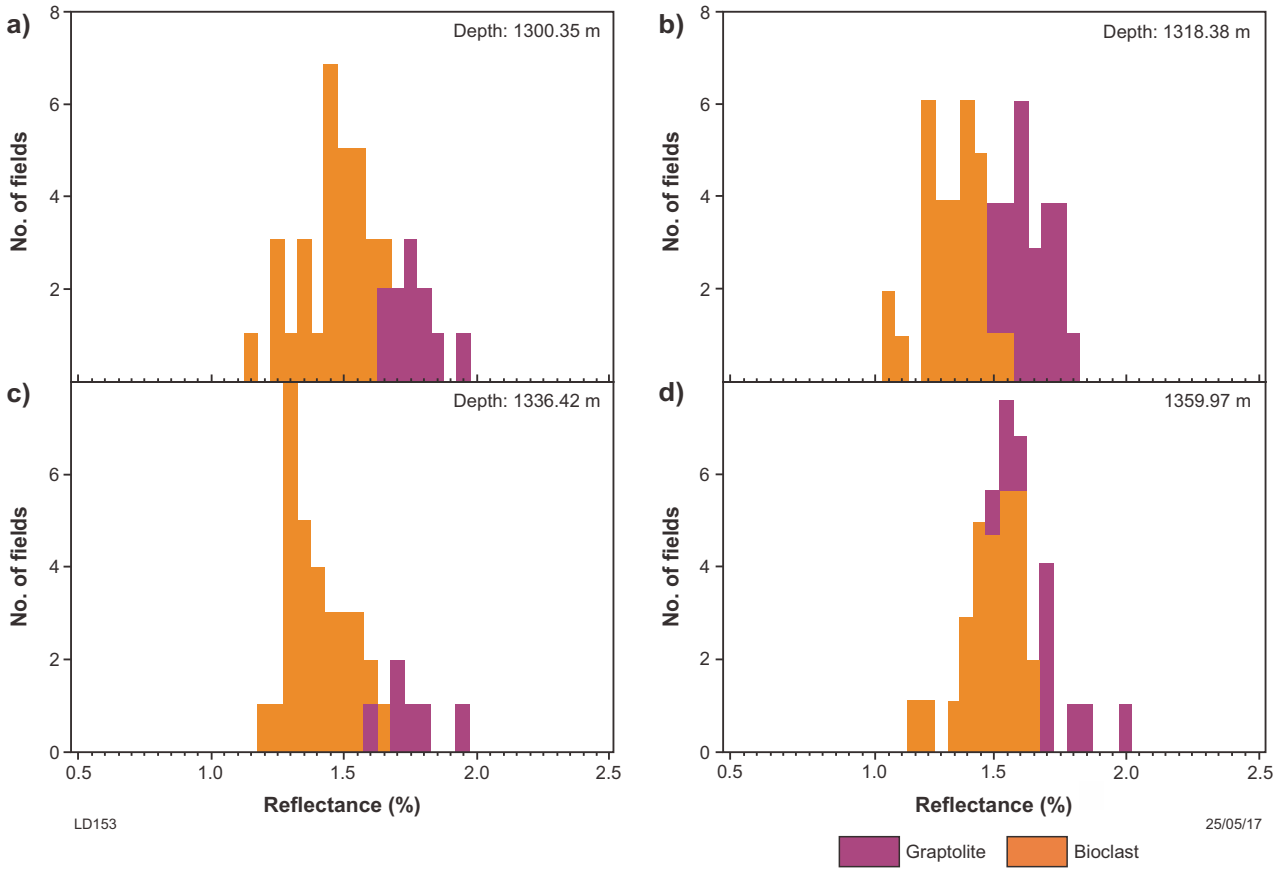

Figure 10. Graptolite and bioclast reflectance distributions: a–d) raw graptolite reflectance (G_{max}) and bioclast reflectance (BC_{max}) histograms from a selection of sample locations in Olympic 1. Distributions are unimodal for both datasets with persistently higher reflectance for graptolite populations and minor overlap between the two populations

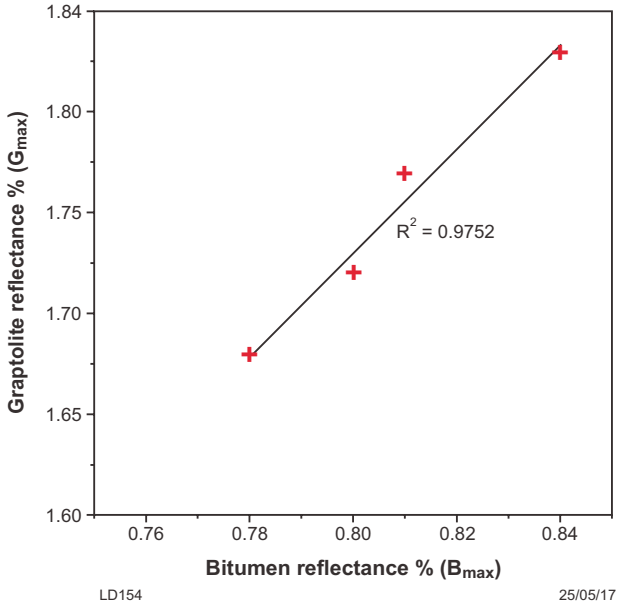

Figure 11. Crossplot of raw bitumen reflectance (B_{max}) and graptolite reflectance (G_{max}) from samples in the Nambeet Formation, Olympic 1. Bitumen is interpreted as in situ. There is a strong positive linear correlation ($R^2 \geq 0.97$) of increasing graptolite reflectance with increasing bitumen reflectance

and 2) determine the thermal maturity and the equivalent phase of hydrocarbon generation. The use of T_{max} as a maturity parameter for the Olympic 1 core samples was documented by Normore and Dent (2017). That work identified a large proportion of the samples as unsuitable for determining maturity because the T_{max} values were supressed by contamination of free hydrocarbon (S_1). Those T_{max} results that are deemed to be reliable plot in the range 440–448˚C, which is within the oil-generation window (Fig. 13). This maturity range overlaps with the normalized vitrinite reflectance data for the bitumen and bioclast data. However, these temperatures imply that the samples are slightly less mature compared to the bioclast and graptolite data (Fig. 12).

Conversion of T_{max} to TR_o

To more accurately compare the different datasets, T_{max} was converted to a vitrinite equivalent, TR_o. T_{max} data are sensitive to kerogen type and Hackely and Cardott (2016) suggested that existing equations should only be applied to appropriate lithologies. Olympic 1 data have been transformed according to equations from Jarvie et al. (2001), Wust et al. (2013) and Laughrey (2014) (Table 6).

Table 6. T_{max} values converted to vitrinite-equivalent reflectance values (TR_o) using three different equations; see text for details

		Vitrinite-equivalent reflectance (TR_o)		
Depth (m)	*T_{max}*	*Jarvie et al. (2001)*	*Wust et al. (2013)*	*Laughrey (2014)*
1154.87	444	0.832	0.7656	0.9524
1184.1	440	0.76	0.706	0.878
1187.69	441	0.778	0.7209	0.8966
1201.11	442	0.796	0.7358	0.9152
1204.05	440	0.76	0.706	0.878
1204.97	443	0.814	0.7507	0.9338
1215.02	445	0.85	0.7805	0.971
1252.26	447	0.886	0.8103	1.0082
1255.24	444	0.832	0.7656	0.9524
1265.13	440	0.76	0.706	0.878
1274.96	443	0.814	0.7507	0.9338
1282.74	442	0.796	0.7358	0.9152
1295	443	0.814	0.7507	0.9338
1303.56	442	0.796	0.7358	0.9152
1303.95	442	0.796	0.7358	0.9152
1305.42	444	0.832	0.7656	0.9524
1307.71	441	0.778	0.7209	0.8966
1310.59	442	0.796	0.7358	0.9152
1312.1	442	0.796	0.7358	0.9152
1313.96	445	0.85	0.7805	0.971
1318	445	0.85	0.7805	0.971
1318.29	440	0.76	0.706	0.878
1318.38	442	0.796	0.7358	0.9152
1321.47	440	0.76	0.706	0.878
1323.31	442	0.796	0.7358	0.9152
1328.03	444	0.832	0.7656	0.9524
1330.14	442	0.796	0.7358	0.9152
1333.49	440	0.76	0.706	0.878
1336.42	448	0.904	0.8252	1.0268
1337.54	444	0.832	0.7656	0.9524
1341.14	444	0.832	0.7656	0.9524
1347.67	442	0.796	0.7358	0.9152
1349.96	446	0.868	0.7954	0.9896

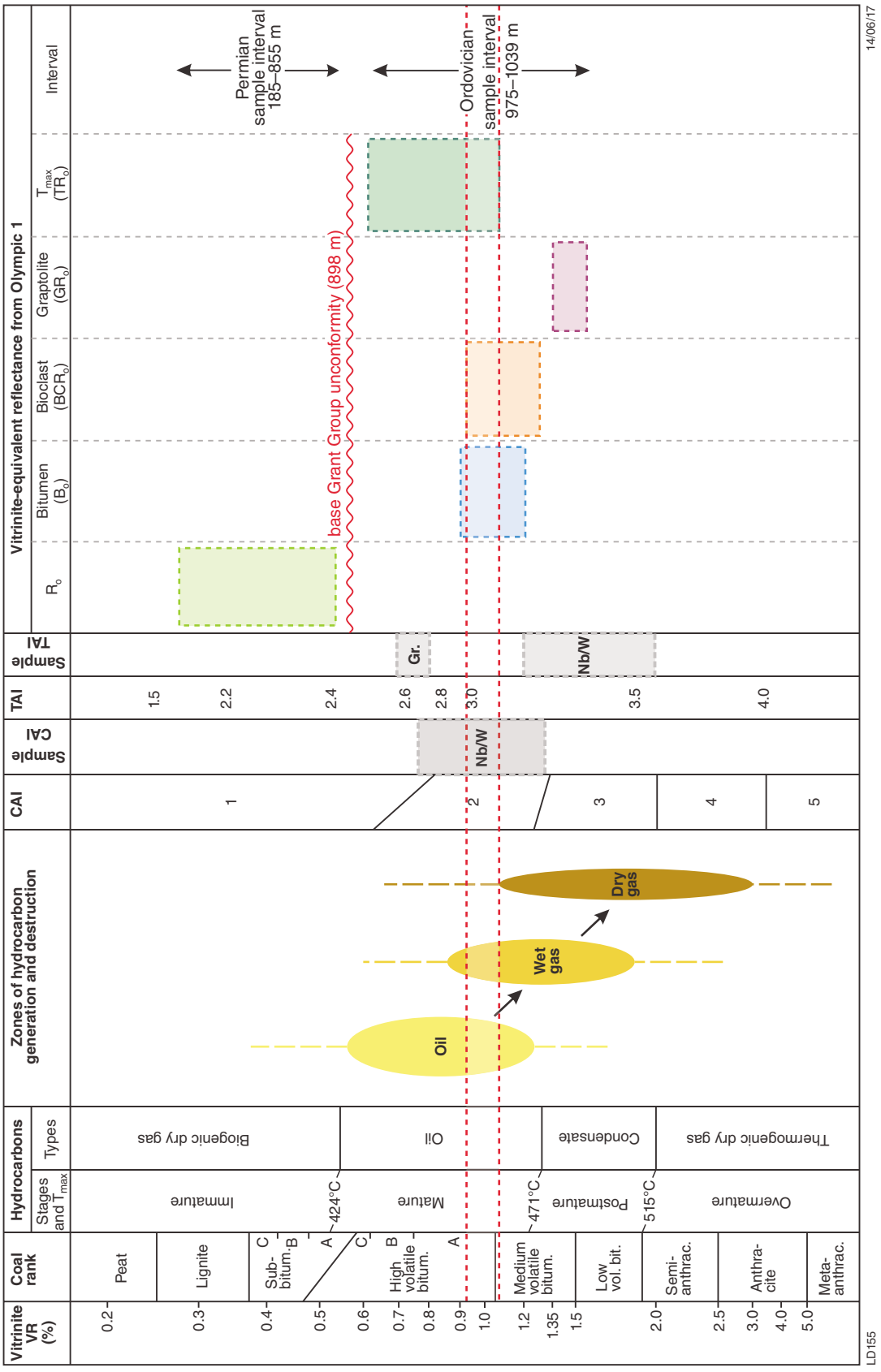

Figure 12. Thermal maturity and hydrocarbon product estimated from converted vitrinite reflectance values. Correlated ranges of hydrocarbon products for R_o values according to a range of studies; figure adapted from Hartkopf-Fröder et al. (2015). R_o range for vitrinite, vitrinite-equivalent bitumen, bioclast, and graptolite data displayed on the right. The zone of agreement within dashed red lines indicates the overlap in reflectance data between datasets. Sample CAI and sample TAI columns show the results of thermal maturities derived from conodonts and spore pollen in Olympic 1, respectively; these relate directly to the adjacent CAI and TAI numerical scales. Abbreviations: Gr., Grant Group; Nb/W, Nambeet and Willara Formations

Jarvie et al. (2001) developed the following equation for the Barnett Shale, which is predominantly a Type II kerogen play (Bruner and Smosna, 2011):

$$TR_o\ (\%) = 0.0180(T_{max}) - 7.16 \qquad \text{(Eq. 13)}$$

Jarvie et al. (2001) noted that the equation was developed excluding Type I kerogens, and is not suitable for conversion of sample points where S_2 is limited.

Wust et al. (2013) developed the following equation for the mixed mudstone–limestone Duvernay Formation of Alberta, a shale-gas play that records Type I/II kerogens (Requejo et al., 1992; Van de Wetering et al., 2016):

$$TR_o\ (\%) = 0.0149(T_{max}) - 5.85 \qquad \text{(Eq. 14)}$$

Laughrey (2014) developed the following equation for the Barnett and Woodford shales:

$$TR_o = 0.0186(T_{max}) - 7.306 \qquad \text{(Eq. 15)}$$

TR_o compared to BR_o, GR_o and BCR_o

TR_o values from the three conversion methods range from 0.706 to 1.02% and there is no significant correlation between TR_o and depth (Fig. 14). There is little difference between the results using equation 13 (TR_o varies from 0.76 to 0.90%) and equation 14 (TR_o varies from 0.70 to 0.83%.), but the conversion of T_{max} to TR_o using equation 15 gives slightly higher TR_o values in the range 0.88 – 1.03% (Fig.14). According to Hartkopf-Fröder et al. (2015), these values lie within the peak oil to early wet-gas phase of maturity. These results show some overlap with the vitrinite-equivalent bitumen and bioclast reflectance (Fig. 12) but do not conform with vitrinite-equivalent graptolite reflectance values.

Other direct visual measures of thermal maturity

Colour alteration index for conodonts

The colour alteration index (CAI) is a numerical measure of the progressive change in colouration of conodont fossils with increasing thermal maturity. This indexing system uses classes or colour intervals for which each interval represents a range of temperatures (Hartkopf-Fröder et al., 2015).

Conodont samples recovered from the cored section in Olympic 1 were well preserved and recorded CAI from 1.5 to 2 (Yong Yi Zhen, 2017, written comm., 18 January). This equates to vitrinite reflectance values ranging from 0.7 to 1.3% (Epstein et al., 1977) and is consistent with the equivalent reflectance values recorded from T_{max}, bitumen and bioclast datasets (Fig. 12).

Thermal alteration index

Thermal alteration index (TAI) is a numerical measure of the progressive change in colouration of spore and pollen grains with increasing thermal maturity. Colouration classification ranges from translucent or pale yellow (pre-hydrocarbon generation) to black (over mature).

Palynological samples were collected in Olympic 1 throughout the cored section of the Ordovician Nambeet Formation (1189.22 – 1432.69 m), and from cuttings in the overlying Permian–Carboniferous Grant Group (760–855 m) (Table 7). Samples from the Grant Group recorded a TAI of 2.6 – 2.7 indicating maturity in the peak oil window. These data are inconsistent with the vitrinite reflectance data at 760–855 m in the Grant Group, which indicates this interval lies within the immature to very early oil-generation window, whereas palynology indicates maturity in the main oil to early wet-gas zone.

Nambeet Formation TAI was measured according to the Pearson (1984) scheme and recorded a TAI range of 3+ to 4–. These values equate to a vitrinite reflectance of 1.2 – 2.0% (Dembicki, 2016) and indicate maturities in the peak wet-gas to dry-gas generation stages. In the Nambeet Formation, vitrinite-equivalent reflectance data expressed as BR_o, BCR_o and TR_o suggest maturity in the peak-oil to wet-gas window. Thus, TAI for this interval suggests a higher maturity more consistent with the GR_o maturity calculation (Fig. 12).

The TAI values indicate that Nambeet Formation samples are significantly more mature than those recorded from the Grant Group, showing the same abrupt increase in maturity below the unconformity as the R_o, BR_o, and BCR_o data. This information is consistent with that recorded from the other datasets.

Regional thermal maturity correlations

A recent regional analysis of Ordovician source-rock samples in the Canning Basin, which contain both oil-prone and oil- and gas-prone kerogen, identified fair to excellent generating potential (Ghori, 2013). The range of interpreted thermal maturity was between immature and the wet-gas generation zones, with most data points lying inside the oil window. The majority of the samples analysed in that study were from the middle Ordovician Goldwyer Formation; therefore, it would be expected that the lower Ordovician Nambeet Formation is more mature.

Ghori (2013) also found the majority of Permian sedimentary rocks to be immature, and that a minority are mature in the lower end of the oil window. These results are broadly consistent with the Grant Group data from Olympic 1.

Geochemical data are available for the Nambeet Formation in 30 wells in the Canning Basin, of which 20 have Rock-Eval data (Table 8). Three of these wells, Nicolay 1, Gap Creek 1 and Tappers Inlet 1, have T_{max} data that can be used to estimate thermal maturity.

Only three of these samples are interpreted to be uncontaminated and these plot as immature or mature, and are therefore suitable to be converted to vitrinite-equivalent reflectance. All three samples were converted

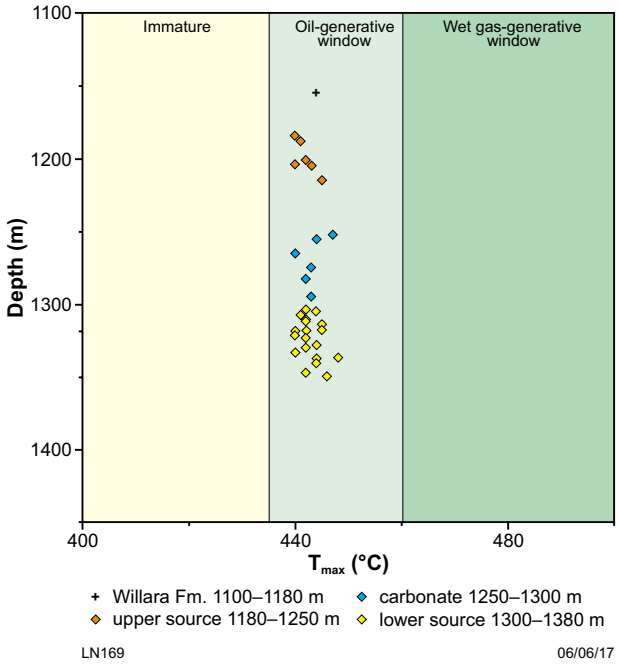

Figure 13. Reliable T_{max} values from Olympic 1 cored section. T_{max} values plot between 440 and 448˚C within the oil generation window. Adapted from Normore and Dent (2017)

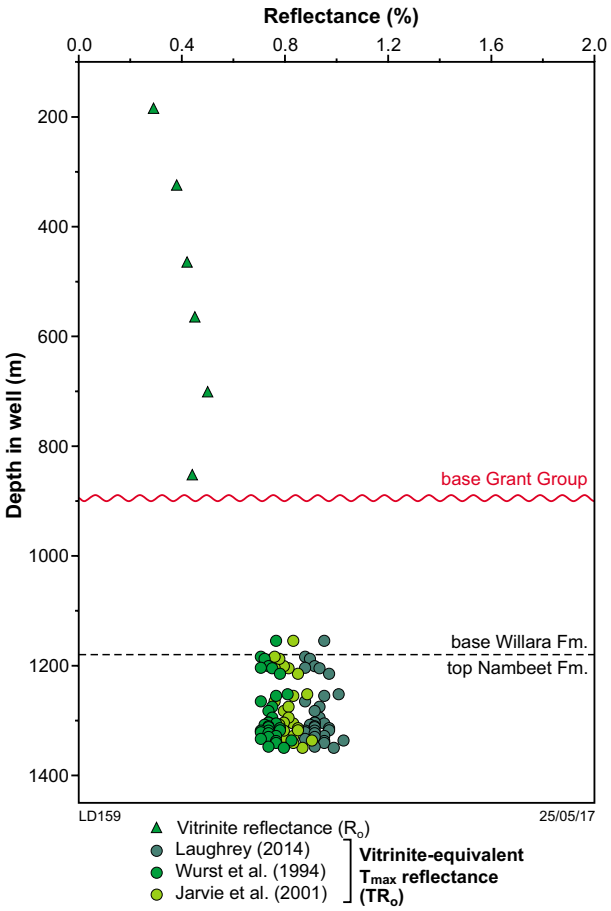

Figure 14. T_{max} converted to vitrinite-equivalent reflectance values (TR_o). Values range from 0.706 to 1.04% when transformed using equations proposed by Jarvie et al. (2001), Wust et al. (2013) and Laughrey (2014)

Table 7. Summary of results from palynological sampling in Olympic 1 including age, colour, and equivalent thermal maturity. Classification scheme MGP refers to the in-house classification scheme of Morgan Goodall Palaeo (Hannaford, 2016)

Depth in well (m)	*Formation*	*Sample Type*	*Age*	*Classification*	*Classification Scheme*	*R_o equivalent*	*Thermal maturity*
760–855	Grant Group	Cuttings	Permian–Carboniferous	2.6 – 2.7	MGP	unknown	Main oil – early wet-gas condensate
1189.22 – 1432.69	Nambeet Formation	Core	Middle Ordovician	3+ to 4–	Pearson (1984)	1.2 – 2.0	Late-mature liquid to early dry gas

using the equations of Wust et al. (2013), Jarvie et al. (2001) and Laughrey (2014), using the same process as the samples from Olympic 1 (Table 9). The derived TR_o values from the Nicolay 1 sample were unrealistically low (including a negative value), given the current burial depth of 3296 m, and data from this well were deemed unreliable (Table 9). The remaining two samples from Gap Creek 1 and Tappers Inlet 1 recorded TR_o values between about 0.65 and 0.84% correlating to the oil-generation maturity window. This is similar to the TR_o range of 0.706 – 1.02% calculated for Olympic 1. This comparison does not take into account the fact that these wells are located in different structural subdivisions of the Canning Basin and are likely to have had different burial histories.

Table 8. Wells in the Canning Basin that contain geochemical information on the Nambeet Formation showing the availability of Rock-Eval data and reliability of T_{max} data for these wells

Well	*Rock-Eval*	*Reliable T_{max}*
BHP PCD 158	X	
BHP PHD 001	X	
Calamia 1	X	
Contention Heights 1	X	
Crystal Creek 1	–	
Dodonea 1	X	
Edgar Range 1	X	
Frankenstein 1	–	
Gap Creek 1	X	X
Goldwyer 1	X	
Grevillea 1	–	
Hedonia 1	X	X
Hilltop 1	X	
Justago 1	X	
Kidson 1	X	
Leo 1	–	
McLarty 1	X	
Mirbelia 2	–	
Nicolay 1	X	X
Olympic 1	X	
Pegasus 1	–	
Percival 1	–	
Pictor 1	X	
Sally May 2	–	
Samphire Marsh 1	–	
Solanum 1	–	
Tappers Inlet 1	X	X
Thangoo 1A	X	
Willara 1	X	
Wilson Cliffs 1	X	

Conclusions

In the absence of vitrinite, which is a standard thermal maturity indicator, other organic components present in the rock, such as bitumen and graptolites, and geochemical indicators (T_{max}) can be used to estimate thermal maturity. Equations developed to convert these organic components into values equivalent to vitrinite are generally situation specific.

The range of vitrinite-equivalent values — BR_o, GR_o, BCR_o and TR_o — derived from each of the four raw reflectance datasets suggests that the thermal maturity of the Nambeet Formation in Olympic 1 was between the peak oil and early dry-gas window. Bitumen, bioclast and T_{max} datasets had the most overlap. The graptolite dataset showed no overlap with the other three datasets and recorded the highest calculated thermal maturity for the formation. Agreement between the T_{max}, bitumen, bioclast and conodont data suggests that the Olympic 1 T_{max} data can provide a reasonable estimate of thermal maturity, but this needs to be assessed in conjunction with other datasets.

Palynological data recovered from the Nambeet Formation were consistent with the graptolite data, suggesting maturity in the wet-gas to dry-gas window. Several datasets need to be used to provide an estimate of maturity. Greatest confidence is given to the bitumen, bioclast and conodont data due to good agreement of results between these datasets and with the T_{max} data.

To better understand the timing and type of generated hydrocarbons from the upper Nambeet shale member, it is crucial to determine the mix of kerogen types present. It is recommended that several complementary analyses for determining kerogen type — including maceral composition, pyrolysis-gas chromatography (Py-GC), extraction of organic matter (EOM), and kerogen kinetics — should be used. Further analyses of the maturity of this source interval from wells in other structural elements of the Canning Basin will assist with future basinwide burial history studies.

Table 9. Reliable T_{max} from the Nambeet Formation from three wells in the Canning Basin and conversion of this T_{max} to vitrinite-equivalent reflectance values according to the equations of Wust et al. (2013), Jarvie et al. (2001) and Laughrey (2014)

			Vitrinite-equivalent reflectance (TR_o)		
Well	*Depth in well (m)*	*T_{max} (˚C)*	*Wust et al. (2013)*	*Jarvie et al. (2001)*	*Laughrey (2014)*
Gap Creek 1	1218	436	0.6464	0.688	0.8036
Nicolay 1	3296	397	0.0653	–0.014	0.0782
Tappers Inlet 1	2243.4	438	0.6762	0.724	0.8408

References

Ardakani, OH, Sanei, H, Lavoie, D, Chen, Z and Mechti, N 2014, Thermal maturity and organic petrology of the Upper Ordovician Utica and Lorraine shales, southern Quebec, Canada: GeoConvention 2014, Calgary, Alberta, Canada, 12 May 2014, p. 1–5.

Barker, CG 1979, Organic geochemistry in petroleum exploration: American Association of Petroleum Geologists, AAPG Continuing Education Course Notes Series 10, 159p.

Bertrand, R 1990, Correlations among the reflectances of vitrinite, chitinozoans, graptolites and scolecodonts: Organic Geochemistry, v. 15, no. 6, p. 565–574.

Bertrand, R 1993, Standardization of solid bitumen reflectance to vitrinite in some Paleozoic sequences of Canada: Energy Sources, v. 15, p. 269–287.

Bertrand, R and Malo, M 2001, Source rock analysis, thermal maturation and hydrocarbon generation in the Siluro-Devonian rocks of the Gaspé Belt basin, Canada: Bulletin of Canadian Petroleum Geology, v. 49, no. 2, p. 238–261.

Bertrand, R and Malo, M 2012, Dispersed organic-matter reflectance and thermal maturation in four hydrocarbon exploration wells in the Hudson Bay Basin: regional implications: Geological Survey of Canada, Open File 7066, 52p.

Bruner, KR and Smosna, R (compilers) 2011, A comparative study of the Mississippian Barnett Shale, Fort Worth Basin, and Devonian Marcellus Shale, Appalachian Basin: US Department of Energy, National Energy Technology Laboratory, DOE/NETL-2011/1478, 118p.

Cole, GA 1994, Graptolite-chitinozoan reflectance and its relationship to other geochemical maturity indicators in the Silurian Qusaiba Shale, Saudi Arabia: Energy & Fuels, v. 8, p. 1443–1459.

Dembicki, H 2016, Source rock evaluation, in Practical petroleum geochemistry for exploration and production: Elsevier, The Netherlands, p. 61–133.

Dow, WG 1977, Kerogen studies and geological interpretations: Journal of Geochemical Exploration, v. 7, p. 79–99.

Epstein, AG, Epstein, JB and Harris, LD 1977, Conodont colour alteration; an index to organic metamorphism: US Government Printing Office, US Geological Survey Professional Paper 995, 27p.

Espitalié, J, Deroo, G and Marquis, F 1985, Rock-Eval pyrolysis and its applications (Part Two): Oil and Gas Science and Technology, v. 40, no. 6, p. 755–784

Gentzis, T and Goodarzi, F 1990, A review of the use of bitumen reflectance in hydrocarbon exploration with examples from Melville Island, Arctic Canada, in Applications of thermal maturity studies to energy exploration edited by VF Nuccio and CE Barker: AAPG Datapages, Rocky Mountain Section Society of Economic Paleontologists and Mineralogists, p. 23–36.

Ghori, KAR 2013, Petroleum geochemistry and petroleum systems modelling of the Canning Basin, Western Australia: Geological Survey of Western Australia, Report 124, 33p.

Guppy, DJ and Opik, AA 1950, Discovery of Ordovician rocks, Kimberley Division: Australian Journal of Science, v. 12, p. 205–206.

Hackley, PC and Cardott, BJ 2016, Application of organic petrography in North American shale petrolem systems: a review: International Journal of Coal Geology, v. 163, p. 8–51.

Hannaford, C 2016, A palynological analysis of Olympic 1, Canning Basin, Western Australia: prepared for Department of Mines and Petroleum, unpublished report, 9p.

Hartkopf-Fröder, C, Königshof, P, Littke, R and Schwarzbauer, J 2015, Optical thermal maturity parameters and organic geochemical alteration at low grade diagenesis to anchimetamorphism: a review: International Journal of Coal Geology, v. 150–151, p. 74–119.

Hunt, JM 1996, Petroleum geochemistry and geology: W.H. Freeman, New York, US, 743p.

International Commission on Stratigraphy 2013, International Chronostratigraphic Chart — v2016/10 update: <www.stratigraphy.org/ICSchart/ChronostratChart2016–10.pdf>.

Jacob, H 1989, Classification, structure, genesis and practical importance of natural solid oil bitumen (migrabitumen): International Journal of Coal Geology, v. 11, p. 65–79.

Jarvie, DM, Claxton, B, Henk, B and Breyer, J 2001, Oil and shale gas from the Barnett Shale, Ft Worth Basin, Texas: AAPG National Convention, Denver, Colorado, 3–6 June 2001, <www.searchanddiscovery.com/abstracts/html/2001/annual/abstracts/0386.htm>.

Karajas, J and Taylor, D 1983, Eagle et al. Aquila No 1 completion report; Eagle Corp: Geological Survey of Western Australia, Statutory petroleum exploration report, W2240A3 (P&A), 176p.

Landis, CR and Castaño, JR 1995, Maturation and bulk chemical properties of a suite of solid hydrocarbons: Organic Geochemistry, v. 22, no. 1, p. 137–149.

Laughrey, CD 2014, Introductory geochemistry for shale gas, condensate-rich shales and tight oil reservoirs: URTeC Annual Meeting Short Course, Denver, Colorado, US, August 2014, 325p.

Link, CM, Bustin, RM and Goodarzi, F 1990, Petrology of graptolites and their utility as indices of thermal maturity in lower Paleozoic strata in northern Yukon, Canada: International Journal of Coal Geology, v. 15, no. 2, p. 113–135.

McTavish, RA 1969, Gap Creek Formation, Canning Basin, Western Australia (Preliminary report of microfauna, age and correlation): West Australian Petroleum Pty Limited, unpublished report, 27p.

Nicoll, RS 1993, Ordovician conodont distribution in selected petroleum exploration wells, Canning Basin, Western Australia: Australian Geological Survey Organisation, Record 1993/17, 136p.

Normore, LS and Dent, LM 2017, Petroleum source potential of the Ordovician Nambeet Formation, Canning Basin: evidence from petroleum well Olympic 1: Geological Survey of Western Australia, Report 169, 20p.

Pearson, DL 1984, Pollen/spore color “standard” version #2: Phillips Petroleum Company, Exploration Projects Section, Bartlesville, Oklohoma, unpublished company file.

Petersen, HI, Schovsbo, NH and Nielsen, AT 2013, Reflectance measurements of zooclasts and solid bitumen in lower Paleozoic shales, southern Scandinavia: correlation to vitrinite reflectance: International Journal of Coal Geology, v. 114, p. 1–18.

Requejo, AG, Gray, NR, Freund, H, Thomann, H, Melchior, MT, Gebhard, LA, Bernardo, M, Pictroski, CF and Hsu, CS 1992, Maturation of petroleum source rocks. 1. Changes in kerogen structure and composition associated with hydrocarbon generation: Energy & Fuels, v. 6, p. 203–214.

Sanei, H, Haeri-Ardakani, O, Wood, JM and Curtis, ME 2015, Effects of nanoporosity and surface imperfections on solid biotumen reflectance (BRo) measurements in unconventional reservoirs: International Journal of Coal Geology, v. 138, p. 95–102.

Schoenherr, J, Littke, R, Urai, JL, Kukla, PA and Rawahi, Z 2007, Polyphase thermal evolution in the Infra-Cambrian Ara Group (South Oman Salt Basin) as deduced by maturity of solid reservoir bitumen: Organic Geochemistry, v. 38, no. 8, p. 1293–1318.

Tissot, BP and Welte, DH 1978, Petroleum formation and occurrence: A new approach to oil and gas exploration: Springer-Verlag, Berlin, 699p.

Van de Wetering, N, Sanei, H and Mayer, B 2016, Organic matter characterization in mixed hydrocarbon producing areas within the Duvernay Formation, Western Canada Sedimentary Basin, Alberta: International Journal of Coal Geology, v. 156, p. 1–11.

Wilkins, RWT 1999, The problem of inconsistency between thermal maturity indicators used for petroleum exploration in Australian Basins: AGSO Journal of Australian Geology and Geophysics, v. 17, no. 5–6, p. 67–76.

Wust, RAJ, Nassichuk, BR, Brezovski, R, Hackley, PC and Willment, N 2013, Vitrinite reflectance versus pyrolysis Tmax data: assessing thermal maturity in shale plays with special reference to the Duvernay shale play of the Western Canadian Sedimentary Basin, Alberta, Canada, in Society of Petroleum Engineers Unconventional Resources Conference Exhibition Paper 167013: Asia–Pacific, Brisbane, Australia, 11p.

Xianming, X, Wilking, RWT, Dehan, L, Zufa, L and Jaimu, F 2000, Inverstigation of thermal maturity of lower Palaeozoic hydrocarbon source rocks by means of vitrinite-like maceral reflectance — a Tarim Basin case study: Organic Geochemistry, v. 31, p. 1041–1052.

In the absence of vitrinite, bitumen and zooclasts are used to derive vitrinite-equivalent reflectance values for the Ordovician Willara and Nambeet Formations in the Olympic 1 petroleum well, Canning Basin. This Report presents and evaluates methodologies for transforming bitumen and zooclast raw reflectance data to vitrinite-equivalent values. Zooclast and bitumen data are compared to T_{max} data, also converted to vitrinite-equivalent values, to check the reliability of the converted datasets. Combined, the bitumen, zooclast and T_{max} data, and additional CAI and TAI data, provide an estimate for thermal maturity for the Nambeet Formation in the Olympic 1 well. Greatest confidence is given to the bitumen, Bioclast 1, conodont and T_{max} data that suggest thermal maturity in the mature oil to early wet-gas zones.

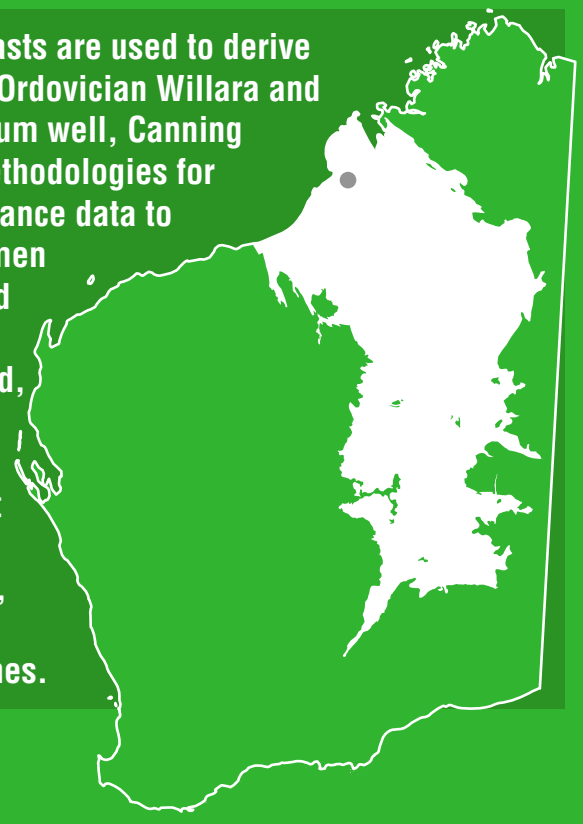

DENT AND NORMORE

ASSESSMENT OF THERMAL MATURITY USING BITUMEN, GRAPTOLITE AND BIOCLAST REFLECTANCE: ORDOVICIAN NAMBEET FORMATION, OLYMPIC 1, CANNING BASIN

REPORT 170

Further details of geological products and maps produced by the Geological Survey of Western Australia are available from:

Information Centre
Department of Mines and Petroleum
100 Plain Street
EAST PERTH WA 6004
Phone: (08) 9222 3459 Fax: (08) 9222 3444

www.dmp.wa.gov.au/GSWApublications